

See discussions, stats, and author profiles for this publication at: <https://www.researchgate.net/publication/282292137>

Light and nutrient co-limitation of phytoplankton communities in a large reservoir: Lake Diefenbaker, Saskatchewan, Canada

Article in *Journal of Great Lakes Research* · November 2015

DOI: 10.1016/j.jglr.2015.10.001

CITATIONS

24

READS

293

8 authors, including:



Rebecca L. North
University of Missouri

36 PUBLICATIONS 588 CITATIONS

[SEE PROFILE](#)



Paul Dubourg
UiT The Arctic University of Norway

4 PUBLICATIONS 39 CITATIONS

[SEE PROFILE](#)



Kristine Hunter
University of Saskatchewan

5 PUBLICATIONS 61 CITATIONS

[SEE PROFILE](#)



Greg Silsbe
University of Maryland Center for Environmental Science

33 PUBLICATIONS 496 CITATIONS

[SEE PROFILE](#)

Some of the authors of this publication are also working on these related projects:



Sensitivity of polar cod early life stages to a changing Arctic: A study of the impact of petroleum and elevated temperature (Sens2Change) [View project](#)



Lake Simcoe [View project](#)



Contents lists available at ScienceDirect

Journal of Great Lakes Research

journal homepage: www.elsevier.com/locate/jglr

Light and nutrient co-limitation of phytoplankton communities in a large reservoir: Lake Diefenbaker, Saskatchewan, Canada

Paul Dubourg^{a,b,1,2}, Rebecca L. North^{a,b,*}, Kristine Hunter^{a,b}, David Vandergucht^{a,b,3}, Oghenemise Abirhire^{a,b}, Greg M. Silsbe^c, Stephanie J. Guildford^{d,e}, Jeff J. Hudson^{a,b}

^a Dept. of Biology, University of Saskatchewan, Saskatoon, SK S7N 5E2, Canada

^b Global Institute for Water Security, University of Saskatchewan, Saskatoon, SK S7N 3H5, Canada

^c Dept. of Botany and Plant Pathology, Oregon State University, 2701 SW Campus Way, Corvallis, OR 97331, United States

^d Emeritus, Dept. of Biology, University of Minnesota, Duluth 2205 East 5th St., Duluth, MN 55812 2401, United States

^e Emeritus, Large Lakes Observatory, University of Minnesota, Duluth 2205 East 5th St., Duluth, MN 55812 2401, United States

ARTICLE INFO

Article history:

Received 14 July 2014

Accepted 31 August 2015

Available online xxxx

Communicated by John-Mark Davies

Keywords:

Algae

Nutrient limitation

Light limitation

Reservoir

Photosynthetic efficiency

Phosphorus

ABSTRACT

The reliance on reservoirs to meet global water demands is increasing, as is the need to develop an understanding of factors influencing water quality in these understudied water bodies. This study assessed how the interaction between light and nutrients influences phytoplankton dynamics in a large, heterogeneous prairie reservoir; Lake Diefenbaker, Saskatchewan. A multiple indicator assessment of factors (light, phosphorus [P], and nitrogen [N]) influencing phytoplankton biomass, physiology, and gross primary productivity (GPP) was conducted. Light deficiency was assessed through the application of an indicator threshold for the mean daily mixed layer irradiance as well as the ratio of this irradiance to the light saturation parameter derived from photosynthesis-irradiance curves. Short-term physiological assays and long-term compositional nutrient status indicators were applied to assess the in situ nutrient deficiency of the epilimnetic phytoplankton communities. We observed regional differences in light conditions and nutrient chemistry related to incoming flow and nutrient load from the South Saskatchewan River. Light deficiency was detected 59% of the times measured during the open-water season of 2013. Both GPP and quantum efficiency of photosystem II (Φ_{PSII}) were relatively high ($108 \pm 101 \text{ mmol O}_2 \text{ m}^{-2} \text{ day}^{-1}$ and 0.57 ± 0.07 , respectively) across all regions and months. During conditions of light sufficiency, there was no evidence of N deficiency, and P was the limiting nutrient to phytoplankton communities 90% of the times measured. Nutrient use efficiency and GPP rates were significantly higher under light sufficient conditions. The asynchrony of light and nutrient supply influences production and biomass accrual in this reservoir.

© 2015 Published by Elsevier B.V. on behalf of International Association for Great Lakes Research.

Introduction

There is considerable debate over the relative importance of phosphorus (P) and/or nitrogen (N) as limiting nutrients in freshwater ecosystems (Conley et al., 2009; Schindler, 2012). The issue is even more complex in inland waters where turbidity may affect the under-water light environment experienced by pelagic phytoplankton. Previous work has shown that the availability of light, or photosynthetically active radiation (PAR), is an important factor limiting phytoplankton growth and primary production in freshwater systems (Guildford et al., 2000; Hecky and Guildford, 1984; Thrane et al., 2014). The light-

dependent process of photosynthesis by primary producers generates energy used for nutrient uptake and assimilation (Beardall et al., 2001). Therefore, as defined by Sterner et al. (1997), nutrient use efficiency by phytoplankton communities is the balance between the growth-limiting resources: light and nutrients. As a result, phytoplankton communities experiencing light deficient conditions can display a lack of response to potential limiting nutrients (Hecky and Guildford, 1984; Venables and Moore, 2010).

The forms of nutrients available for phytoplankton assimilation also affect nutrient use efficiency. Nutrient bioavailability refers to those fractions of the total mass of P or N that are readily assimilable by organisms (i.e., dissolved inorganic), or are made more assimilable through the activities of the organisms themselves (i.e., production of phosphatases). It can also include the portion of the total mass which has been assimilated and is already intracellular (i.e., luxury consumption; Reynolds and Davies, 2001). Nutrient use by phytoplankton communities is directly related to the forms available and the differential energy requirements for their uptake; thus, water column nutrient concentrations do not relate directly to nutrient bioavailability to phytoplankton

* Corresponding author at: Dept. of Biology, University of Saskatchewan, Saskatoon, SK S7N 5E2, Canada.

E-mail address: rebeccanorth@gmail.com (R.L. North).

¹ Dept. of Arctic and Marine Biology, UiT The Arctic University of Norway, 9037 Tromsø, Norway.

² P. Dubourg and R.L. North have contributed equally to this manuscript.

³ Saskatchewan Water Security Agency, Regina, SK, Canada, S4P 4K1.

communities (Hecky and Kilham, 1988). It is preferable that the in situ nutrient deficiency of phytoplankton be assessed with a variety of nutrient status indicators that reflect the community response to nutrients (Davies et al., 2004; Guildford et al., 2005; Healey and Hendzel, 1979a). Variations in nutrient limitation and the selective advantages and disadvantages incurred among species are among the fundamental controls on primary production and community composition (Tilman, 1976). In this study, we are specifically interested in the immediate needs of the extant plankton community and limitation of their growth rates (Blackman limitation; Blackman, 1905). We define nutrient deficiency as a control on the instantaneous growth (by proxies for phytoplankton biomass: chlorophyll *a* [Chl *a*] and sestonic carbon [C] concentrations) of phytoplankton and their photosynthetic response (i.e., maximum quantum yield of photosystem II [Φ_{PSII}] and photosynthesis–irradiance [P–E] parameters) to nutrients. Given the complex nature of these communities, strength lies in the utilization of multiple indicators (lines of evidence) to diagnose factors limiting phytoplankton growth rates. Our application of physiological indicators aims to identify light and nutrient deficiency at proximate scales (Davies et al., 2010; Healey, 1975). We define co-limitation as the simultaneous limitation of growth rate by light and a nutrient; explained by the ability of an increased supply of light or nutrients to compensate for the decreased supply of the other (Healey, 1985). This reciprocal relationship between light and nutrients can regulate the ability of phytoplankton to cope with low-light conditions through physiological adjustments such as the synthesis of new pigments (e.g., Chl *a*) to capture light, balancing photosynthesis with photo-protection, repair, and accrual of biomass (Falkowski and Raven, 2007; Kirk, 1994). Consequently, light availability modifies nutrient assimilation and use by primary producers (Sterner et al., 1997) uncoupling the relationship between limiting nutrient supply and potential for maximal rates of growth, biomass accrual, and gross primary productivity.

The interaction between light and nutrients is very prevalent in river-valley reservoirs where inflowing river water causes turbidity fluctuations that necessitate rapid physiological responses of the in situ phytoplankton communities. Given the globally increasing construction of dams (Zarfl et al., 2015), it is imperative that we develop an understanding of factors influencing algal biomass and productivity in these important but understudied water bodies. Our study was conducted on one of the largest reservoirs in the world (Lehner et al., 2011): Lake Diefenbaker (LD), Saskatchewan, Canada. Using LD as a model system on which to test the reservoir continuum concept (Kimmel and Groeger, 1984), we assessed phytoplankton nutrient use efficiency along its length. The reservoir continuum concept delineates three regions within river-valley reservoirs as up-reservoir riverine, to transition, and finally to lacustrine regions near the dams. This concept hypothesizes that as river-reservoirs transition from inflowing upstream regions to downstream lacustrine regions nutrients decrease and light availability increases. Thus, we would assume that the phytoplankton communities are experiencing spatially differential light and nutrient influences on their growth and productivity, on an up-reservoir to dam gradient. Knowledge gained on LD can be applied to other increasingly important reservoirs on a global basis.

Lake Diefenbaker is a mesotrophic, dimictic, multi-purpose reservoir that provides a number of services including flood protection, hydro-power generation, recreation, irrigation, and industrial and municipal water resources (SWSA, 2012). In the mid-1980s, the reservoir was categorized as meso- or oligo-trophic and P was considered to be the ultimate control on phytoplankton growth (Saskatchewan Environment and Public Safety and Environment Canada [SEPS and EC], 1988). A recent study quantifying the 2008–2011 TP and total nitrogen (TN) loads reported that of the 28 lakes and reservoirs in the Lake Winnipeg basin, LD represents the 5th largest (by volume), with the highest P and N loads (Donald et al., 2015). Although recent TP loads to LD are high (3146

tonnes yr⁻¹), they are ~3.6 times lower than the TN load (11,388 tonnes yr⁻¹; Donald et al., 2015).

We predict that light availability could be an important factor influencing LD's nutrient use efficiency, with implications for phytoplankton biomass and gross primary productivity. Due to the turbid inflow from the SSR (Hudson and Vandergucht, in this issue; Yip et al., in this issue), we predict that the underwater light environment is lowest up-reservoir and increases towards the dams, consistent with the river continuum concept. In order to address light and nutrient co-limitation of LD's phytoplankton communities, we measured phytoplankton biomass, physiology, and GPP in combination with a variety of light and nutrient deficiency indicators throughout the length of the reservoir during the open-water season of 2013. To our knowledge, this study represents the most comprehensive suite of light and nutrient status indicators applied to a freshwater reservoir. The objectives of our study were to 1) assess the presence and degree of light and nutrient (i.e., P and N) co-limitation of LD's phytoplankton communities; 2) determine how nutrient use efficiency influences phytoplankton biomass, physiology, and gross primary production; and 3) examine temporal and spatial differences in interacting factors regulating phytoplankton dynamics within the reservoir continuum concept.

Methods

Study site and field sampling

Lake Diefenbaker is a large reservoir (182 km in length) with a storage capacity of 9 km³ at full supply level (Sadeghian et al., in this issue). Covering an area of 394 km², with a mean depth of 22 m (Sadeghian et al., in this issue), it is the largest source of moderate quality water in southern Saskatchewan (Fig. 1). The major inflow (98%) to LD is the South Saskatchewan River (SSR), originating in the foothills of Alberta's Rocky Mountains. The outflow is mostly through the Gardiner Dam (99%), with the remainder flowing through the Qu'Appelle Dam (SWSA, 2012; Fig. 1). In 2013, heavy rainfalls in southern Alberta (June 19–22) resulted in extreme flooding of up-stream Calgary. As a result, LD experienced a large increase in flow, peaking between late June–early July (Hudson and Vandergucht, in this issue).

A total of 12 sites along LD's main channel were sampled between Highway 4 and the Gardiner and Qu'Appelle Dams (Fig. 1). Sampling of all sites was conducted on a monthly basis from June to mid-October, 2013. Whole water samples were collected from a 2 m depth using a Van Dorn, and a peristaltic pump was used for the collection of total dissolved iron (TDFe) samples employing trace metal clean protocols to reduce metal contamination. Within 12 h of collection, water samples were stored at ambient temperatures in an environmental chamber at the University of Saskatchewan (Saskatoon, SK) until processing.

Physical parameters

A Yellow Springs Instruments sonde (YSI, model 6600 V2) was deployed at each station to collect temperature, turbidity, dissolved oxygen, specific conductance, Chl *a* fluorescence, and depth profiles in one second increments. The thermocline was defined as the depth where changes in water temperature were >0.5 °C m⁻¹. Mixing depth (Z_{mix} , Table 1) was reported as the depth from the water surface to the top of the thermocline and maximum depth (Z_{max}) was based on the 1986 bathymetry (SPMC, ca., 1986). Secchi disk depths were recorded during each sampling event. PAR profiles were measured using a Biospherical BIC compact four-channel radiometer (Biospherical Instruments, San Diego CA) and were used to calculate the vertical attenuation coefficient (K_{dPAR} ; Table 1) from the linear regression of the natural logarithm of irradiance versus depth (Kirk, 1994). Mean daily mixed layer irradiance (\bar{E}_{24} , $\mu\text{mol photons m}^{-2} \text{s}^{-1}$), the mean light

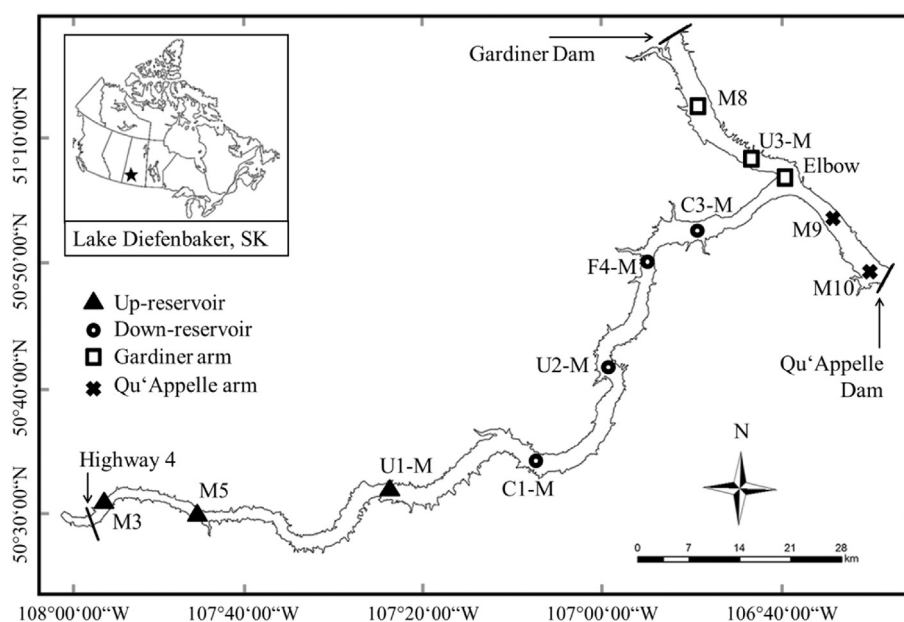


Fig. 1. Map of Lake Diefenbaker (Saskatchewan, Canada) depicting sites sampled in 2013. Sites were located along the main channel of the reservoir and grouped into 4 regions; Up-reservoir, Down-reservoir, Gardiner arm, and Qu'Appelle arm.

Table 1

Definitions, abbreviations, and units describing light, nutrient, and phytoplankton parameters. Superscript B applied to an abbreviation denotes normalization to Chlorophyll *a*.

	Parameter	Abbreviation	Units
Light	Maximum depth	Z_{\max}	Meter
	Mixing depth	Z_{mix}	Meter
	Photosynthetically active radiation	PAR	$\mu\text{mol photons m}^{-2} \text{s}^{-1}$
	Vertical light attenuation coefficient	K_{dPAR}	m^{-1}
	Mean daily mixed layer irradiance	\bar{E}_{24}	$\mu\text{mol photons m}^{-2} \text{s}^{-1}$
	Secchi disk depth	Secchi	Meter
	Mean daily incident irradiance	\bar{E}_0	$\mu\text{mol photons m}^{-2} \text{s}^{-1}$
	Light saturation parameter ($r\text{ETR}_{\max}/\alpha$)	E_k	$\mu\text{mol photons m}^{-2} \text{s}^{-1}$
	Light deficiency threshold	\bar{E}_{24}/E_k	Unitless
	Light utilization efficiency (light limited slope of the P-E curve)	α	Photons reemitted photons absorbed ⁻¹ / $\mu\text{mol photons m}^{-2} \text{s}^{-1}$
	Maximum relative electron transport rate through PSII	$r\text{ETR}_{\max}$	Photons reemitted photons absorbed ⁻¹
	Maximum quantum yield of PSII	ϕ_{PSII}	Unitless
	Daily gross primary production rate	GPP	$\text{mmol O}_2 \text{m}^{-2} \text{day}^{-1}$
	Daily gross primary production rate normalized to Chlorophyll <i>a</i>	GPP^B	$\text{mmol O}_2 (\text{mg Chl } a^{-1}) \text{m day}^{-1}$
	Slope of the GPP^B - \bar{E}_{24} curve	$\text{GPP}^B/\bar{E}_{24}$	$\text{mmol O}_2 (\text{mg Chl } a^{-1}) \text{m day}^{-1}/\mu\text{mol photons m}^{-2} \text{s}^{-1}$
Nutrient	Total phosphorus	TP	$\mu\text{mol L}^{-1}$
	Total dissolved phosphorus	TDP	$\mu\text{mol L}^{-1}$
	Particulate phosphorus	PP	$\mu\text{mol L}^{-1}$
	Dissolved reactive phosphorus	DRP	$\mu\text{mol L}^{-1}$
	Total nitrogen	TN	$\mu\text{mol L}^{-1}$
	Total dissolved nitrogen	TDN	$\mu\text{mol L}^{-1}$
	Particulate nitrogen	PN	$\mu\text{mol L}^{-1}$
	Nitrate	NO_3^-	$\mu\text{mol L}^{-1}$
	Ammonium	NH_4^+	$\mu\text{mol L}^{-1}$
	Total dissolved iron	TDFe	$\mu\text{mol L}^{-1}$
	Dissolved reactive silica	DRSi	$\mu\text{mol L}^{-1}$
	PO_4 turnover time	TT	Minutes
	Phosphorus uptake	P-debt	$\mu\text{mol P } \mu\text{g Chl } a^{-1}$
	Particulate carbon to particulate phosphorus ratio	C:P	Molar ratio
	Particulate nitrogen to particulate phosphorus ratio	N:P	Molar ratio
	Particulate alkaline phosphatase activity	APA	$\text{nmol P } \mu\text{g Chl } a^{-1} \text{min}^{-1}$
	Ammonium uptake	N-debt	$\mu\text{mol NH}_4^+ \mu\text{g Chl } a^{-1}$
	Particulate carbon to particulate nitrogen ratio	C:N	Molar ratio
Phytoplankton	Chlorophyll <i>a</i>	Chl <i>a</i>	$\mu\text{g L}^{-1}$
	Pigment absorption coefficient	a_{ϕ}	$\text{m}^{-2} \text{mg Chl } a^{-1}$
	Particulate organic carbon	POC	$\mu\text{mol L}^{-1}$
	Particulate carbon to chlorophyll <i>a</i> ratio	POC:Chl <i>a</i>	$\mu\text{mol C } \mu\text{g Chl } a^{-1}$
	Total phytoplankton biomass	Phyto	mg m^{-3}
	Phytoplankton biomass to chlorophyll <i>a</i> ratio	Phyto:Chl <i>a</i>	Unitless
	Cryptophyte biomass	Crypto	mg m^{-3}
	Bacillariophyte biomass	Bacill	mg m^{-3}

experienced by a freely circulating algal cell during a 24 hour period was calculated following Guildford et al. (2000):

$$\bar{E}_{24} = \bar{E}_0 \times (1 - \exp(-1 \times K_{dPAR} \times Z_{mix})) \times (K_{dPAR} \times Z_{mix})^{-1} \quad (1)$$

where mean daily incident irradiance (\bar{E}_0) was calculated as the 24 hour average on the sampling date from solar radiation ($W\ m^{-2}$) obtained from a nearby meteorological station (University of Saskatchewan, Saskatoon, SK; <http://www.usask.ca/weather/kfarm/data/>) and scaled to PAR ($\mu mol\ photons\ m^{-2}\ s^{-1}$) using a factor of 2.047 after Kalff (2002).

Water chemistry

Total P (TP), total dissolved P (TDP), dissolved reactive P (DRP), and particulate P (PP; collected on glass fiber filters, GF75, nominal pore size $0.7\ \mu m$) were analyzed according to Parsons et al. (1984) after digestion using the persulfate-oxidation technique for TP, TDP, and PP (Menzel and Corwin, 1965). Concentrations of dissolved nutrients such as TDP, DRP, total dissolved N (TDN), ammonium (NH_4^+), nitrate (NO_3^-), dissolved reactive silica (DRSi), and total dissolved Fe (TDFe) were measured on syringe-filtered whole lake water ($0.2\ \mu m$ polycarbonate filter). NH_4^+ was measured fluorometrically using a Varioskan Flash spectral scanning multimode reader (Thermo Scientific) according to Holmes et al. (1999) with a modified method of standard additions following Taylor et al. (2007). Total N (TN), TDN, and NO_3^- were measured through second derivative spectroscopy (Bachmann and Canfield, 1996; Crumpton et al., 1992). DRSi concentrations were measured colorimetrically (APHA, 1989).

Concentrations of TDFe were measured on filtered lake water acidified with nitric acid (0.2%) prior to analyses. Analyses of TDFe concentrations were conducted on a graphite furnace atomic absorption spectrometer (AAAnalyst 800, Perkin Elmer, USA). Particulate organic C (POC) and particulate N (PN) samples were collected on pre-combusted quartz filters (GF75, nominal pore size $0.39\ \mu m$), dried and stored. Carbonates were removed from the POC filters by fumigation using concentrated hydrochloric acid (37%) in a dessicator for 4 h. The PN samples were non-acidified and thus analyzed independently to POC (Brodie et al., 2011). POC and PN samples were analyzed via an ANCA-GSL sample preparation unit and Tracer 20 mass spectrometer (Europa Scientific).

Phytoplankton biomass and pigment absorption coefficient (a_ϕ)

Sample water was filtered onto glass fiber filters (GF75, nominal pore size $0.7\ \mu m$) for determination of Chl *a* concentrations and filters were frozen until analyses. Chl *a* extraction followed Bergmann and Peters (1980) and Webb et al. (1992) using ethanol as a solvent. Samples were acidified and corrected for phaeophytin (Nusch, 1980) and concentrations were obtained using a spectrophotometer (UV-4201 PC, Shimadzu).

Phytoplankton samples were analyzed on a limited number of samples ($n = 20$) representing three regions of the reservoir; up-reservoir (U1-M), down-reservoir (U2-M and C3-M), and the Gardiner arm (U3-M) over the five month sampling period. Methods are described in Abirhire et al. (in this issue); briefly, samples were preserved with Lugol's iodine and phytoplankton were counted following Utermöhl (1958) using an inverted microscope (Olympus IX51). Phytoplankton were identified to genus with the aid of taxonomic guides (Bellinger and Sigee, 2010; John et al., 2002; Wehr and Sheath, 2003). Phytoplankton cell sizes were obtained through image-Pro Analyser 7.0 computer software and final biomass was calculated by employing Algamica (Version 4.0), a computerized phytoplankton counting program by Gosselain and Hamilton (2000).

The phytoplankton pigment absorption coefficient (a_ϕ) was quantified in parallel with rapid light curve (RLC; described below) measurements using the quantitative filter technique as described in Tassan and Ferrari (1995) and using the calculations described in Silsbe et al.

(2012). Briefly, 100–1500 mL of lake water was passed through a 47 mm GF/F filter and the filter was immediately frozen. The absorbance (350–750 nm) of the particulate matter retained on the filter was then measured on a scanning spectrophotometer (UV-4201 PC, Shimadzu) before (A_P) and after (A_{NAP}) depigmentation with a sodium hypochlorite solution. From these measurements, a_ϕ was calculated using the following formula where 2.303 is the natural logarithm of 10, β is the path-length amplification factor that accounts for the difference between absorption on a filter and water and is equal to 2, and V_f/A_f is the ratio of volume filtered to the clearance area of the filter:

$$a_\phi = 2.303 \times [A_P - A_{NAP}] \times \beta^{-1} \times [V_f/A_f]^{-1} \quad (2)$$

Light dependency of the quantum efficiency of PSII

A Water-Pulse Amplitude Modulated (PAM) fluorometer (Heinz Walz GmbH, Effeltrich Germany) controlled by WinControl software (version 3.22) was used to measure ϕ_{PSII} and perform RLCs to measure the light dependency of ϕ_{PSII} . Whole water samples for measurements of ϕ_{PSII} had a brief exposure to far-red light after 30 min of dark adaptation. Measurements were done in triplicate and corrected for background fluorescence by measuring sample filtrate ($0.2\ \mu m$ polycarbonate filter) in triplicate. Measurements of RLCs were in 8, 1 minute intervals of increasing light intensity (E ; range 3–1461 $\mu mol\ photon\ m^{-2}\ s^{-1}$). Photosynthetic-irradiance (P–E) parameters were derived for each RLC by fitting ϕ_{PSII} against irradiance data to an E-normalized version of Webb et al. (1974) following Silsbe and Kromkamp (2012):

$$\alpha \times E_k \times [1 - e(-E \times E_k)] \times E^{-1} \quad (3)$$

where the light utilization efficiency (α) is defined as the light limited slope of the P–E curve and $rETR_{max}$ is the maximum relative electron transport rate through PSII. The light saturation parameter (E_k) is then defined as $rETR_{max}/\alpha$ or the irradiance that represents the inflection from α to $rETR_{max}$ (Table 1). P–E models that could allow for photoinhibition were unnecessary to describe the data.

Gross phytoplankton production

Gross phytoplankton productivity (GPP) was derived from the RLC P–E parameters, a_ϕ , \bar{E}_0 , and K_{dPAR} using the R package 'phytotoools' that is based on the primary production model described by Fee (1990). Briefly, this approach first constructs the distribution of PAR through the depth and time of day ($E_{z,t}$) as a function of K_{dPAR} and \bar{E}_0 . Then, oxygenic photosynthetic rates (P_{O_2}) are calculated using the following equation where $E_{z,t}$ is expressed in units of $mmol\ photons\ m^{-2}\ s^{-1}$, a_ϕ has units of m^{-1} , $\phi_{PSII}(E)$ represents the RLC P–E parameters and is dimensionless, Φ_{RC} is the quantum yield of photochemistry within PSII ($mol\ e^- [mol\ photons\ absorbed]^{-1}$) and is assumed 1, and Φ_{O_2} is the quantum yield of O_2 evolution ($mol\ O_2 [mol\ e^-]^{-1}$) and assumed to be 0.25.

$$P_{O_2} = E_{z,t} \times a_\phi \times \phi_{PSII}(E) \times \Phi_{RC} \times \Phi_{O_2} \quad (4)$$

Finally, P_{O_2} is integrated through depth and time and multiplied by $1/86400\ s \times day^{-1}$ to arrive at units of $mmol\ O_2\ m^{-2}\ day^{-1}$.

Nutrient status indicators

The nutrient status of the phytoplankton communities were assessed through a variety of indicators including PO_4 turnover times (TT), alkaline phosphatase activity (APA), P- and N-debts, stoichiometric ratios (N:P, C:P, C:N), and photosynthetic efficiency experiments (Tables 1 and 2). TT and APA were measured as described in Vandergucht et al. (2013) using radiophosphate uptake bioassays for

Table 2

Light and nutrient status indicator thresholds applied to phytoplankton communities. Values are from Guildford et al. (2005); P-debt, N-debt, C:N, C:P, and POC:Chl *a* are based on Healey and Hendzel (1979b), TT is based on Lean et al. (1983), and \bar{E}_{24} and E_k on Hecky and Guildford (1984). See Table 1 for parameter definitions and units.

Parameter	Limiting factor	No deficiency	Moderate deficiency	Extreme deficiency	Deficient
\bar{E}_{24}/E_k	Light	>1			<1
\bar{E}_{24}	Light	>41.7			<41.7
TT	P	>60	<60	<6	
P-debt	P	<0.075			>0.075
C:P	P	<129	>129	>258	
N:P	P	<22			>22
N-debt	N	<0.15			>0.15
C:N	N	<8.3	>8.3	>14.6	
POC:Chl <i>a</i>	N/P	<4.2	>4.2	>8.3	

TT. Briefly, carrier-free radiophosphate was added to samples ($^{33}\text{PO}_4$, final activity $\sim 50,000$ cpm mL^{-1}) and planktonic uptake of $^{33}\text{PO}_4$ was monitored by sub-sampling the dissolved pool at approximately 1, 2, 5, 8, and 12 min after radiophosphate addition (syringe filtration, 3–10 mL sub-samples, 25 mm diameter polysulphone, 0.2 mm pore size). Radioactivity was measured by liquid scintillation counting and corrected for background radioactivity; quenching of samples was not detected. Radioactivity remaining in the dissolved fraction (i.e., total disintegrations per minute) over time was fitted to a polynomial function (Currie and Kalf, 1984). The uptake constant was determined by taking the derivative of the polynomial at time zero and dividing by total radioactivity. The reciprocal of the uptake constant is TT. For APA, a 5 μM substrate (4-methylumbelliferyl phosphate; 4-MUP) was added to sample water and measured fluorometrically using a Varioskan Flash spectral scanning multimode reader (Thermo Scientific). Total and dissolved ($<0.2 \mu\text{m}$) APA were measured and subtracted from each other to obtain particulate APA which was standardized to extracted Chl *a* concentrations.

P- and N-debt experiments were based on Healey (1977) and were combined with photosynthetic efficiency experiments. The ϕ_{PSII} of the nutrient spiked water (+N, +P, +N + P) was measured in triplicate, before and after dark incubation. Background fluorescence was again measured as sample water filtrate (0.2 μm polycarbonate filter) and subtracted from ϕ_{PSII} measurements. Each lake sample was divided into 4, 900 mL sub-samples. Three containers received additional nutrients (+N, +P, +N + P; final concentration 5 μM) of NH_4Cl and KH_2PO_4 , respectively. The fourth sub-sample served as a control without nutrient addition. All treatments were incubated in the dark for 18–24 h, in an environmental chamber at in situ temperatures. After incubation, ϕ_{PSII} measurements were again conducted on all 4 treatments. N-debt and P-debt samples were taken from the +N and +P treatments, and uptake was measured as the difference in nutrient concentrations from before and after incubation normalized to Chl *a* concentrations.

Light and nutrient status indicators

The application of phytoplankton physiological deficiency thresholds to a variety of light and nutrient status indicators allows for the critical assessment of deficiencies comparable across natural systems. In most cases, the thresholds (Table 2) were developed and applied to growth rates of freshwater algal batch cultures in laboratory experimental conditions representing nutrient sufficiency and various degrees of P and N limitations (Healey and Hendzel, 1979b) along with light interactions (Rhee and Gotham, 1981). Since their development, the indicators and their associated thresholds have been successfully applied to a diverse global set of lakes ranging in trophic status from eutrophic, light limited Lake Victoria (e.g., Guildford et al., 2003; North et al., 2008), to oligotrophic Lake Superior (e.g., Guildford et al., 2000), and a variety of smaller lakes (e.g., Guildford and Hecky, 2000).

Previous researchers have differentiated between proximate light limitation and light sufficiency through the use of thresholds describing the daily mixed layer irradiance (Hecky and Guildford, 1984; Venables and Moore, 2010). Above these light thresholds, phytoplankton growth rates are assumed to be limited by another factor (i.e., nutrients). We employ such an approach here using the light deficiency thresholds (\bar{E}_{24}/E_k and \bar{E}_{24}) developed on a Canadian reservoir (South Indian Lake, Manitoba; Hecky and Guildford, 1984) and supported by experimental algal culture studies (Rhee and Gotham, 1981). Hecky and Guildford (1984) found that the onset of P deficiency occurred at \bar{E}_{24} values ranging from 41.7 to 58.3 $\mu\text{mol m}^{-2} \text{s}^{-1}$ and attributed the variability to differences in algal composition and mixing depths. The indicator threshold for \bar{E}_{24} was applied to LD to explore light and nutrient co-limitation as it represents the balance between light ($<41.7 \mu\text{mol m}^{-2} \text{s}^{-1}$) and nutrient ($>41.7 \mu\text{mol m}^{-2} \text{s}^{-1}$) deficiency of phytoplankton populations (Table 2; Hecky and Guildford, 1984). The upper range of this threshold (58.3 $\mu\text{mol m}^{-2} \text{s}^{-1}$) has also been applied to western Canadian lakes and reservoirs (Davies et al., 2004). The Hecky and Guildford (1984) threshold is similar to that applied in the high nutrient low chlorophyll regions of the ocean, where a threshold of 35 $\mu\text{mol m}^{-2} \text{s}^{-1}$ was used to assess light limitation of phytoplankton communities (Venables and Moore, 2010). To test the application of the freshwater \bar{E}_{24} (41.7 $\mu\text{mol m}^{-2} \text{s}^{-1}$) threshold's relevance to Lake Diefenbaker, we conducted segmented regression analyses (Muggeo, 2008) on GPP rates and phytoplankton biomass to identify breakpoints in the light environment (\bar{E}_{24}) representing the gradient between light and nutrient deficiency. Our analyses identified breakpoints for GPP and phytoplankton biomass of 26.5 and 43.0 $\mu\text{mol m}^{-2} \text{s}^{-1}$, respectively; with a mean of 34.7 $\mu\text{mol m}^{-2} \text{s}^{-1}$. Within our dataset there were five occurrences where \bar{E}_{24} values fell between the literature established 41.7 and our breakpoint identification at 34.7 $\mu\text{mol m}^{-2} \text{s}^{-1}$, representing 8% of the samples; thus, the application of the lower range of the literature established freshwater threshold (41.7 $\mu\text{mol m}^{-2} \text{s}^{-1}$; Table 2; Hecky and Guildford, 1984) seems valid to our dataset. We acknowledge that this threshold is variable, but it serves as a starting point for discussion and evaluation of our data.

Previously established literature-supported thresholds for nutrient limitation (Healey and Hendzel, 1979b; Guildford et al., 2005; Table 2) were applied to measurements of P-debt, N-debt, C:N, C:P, N:P, and POC:Chl *a* ratios. Healey and Hendzel's (1979b) thresholds were based on experimental culture results and applied in a large lake survey (Healey, 1975). The division points were selected for no deficiency (exponentially-growing algae), moderate deficiency (a growth rate of half the maximum), and extreme deficiency (a growth rate of less than 1/5 the maximum; Healey and Hendzel, 1979b). Healey and Hendzel's (1979b) APA threshold was developed using o-methyl-fluorescein-phosphate (OMFP) as a substrate, and therefore, was not directly applicable to our APA measurements because we used a different substrate (4-MUP).

The strength of nutrient status work is in the application of more than one indicator when evaluating a natural population; thus the Healey and Hendzel (1979b) nutrient indicators were supplemented with an additional P status indicator; an estimate of the turnover time (TT) of phosphate using radiophosphate (Lean et al., 1983). Defined as the time required for phosphate to be taken up, TT provides an indication of the metabolic state of the plankton community (though does not account for phytoplankton or bacterial biomass). The thresholds were defined by differentiating between rapid (6–60 min) TTs indicating that phosphate was in great demand, relative to long TTs (60–12,000 min) indicative of conditions where phytoplankton were not phosphate depleted (Lean et al., 1983).

There is a non-linear relationship between irradiance, growth rates, and photosynthesis, particularly for multi-species assemblages with variable net growth efficiency and POC:Chl *a* ratios (Falkowski and Raven, 2007). Thus, we acknowledge that our application of nutrient (sensu Healey, 1975, 1977, 1985; Healey and Hendzel, 1979a,b) and

light (sensu Hecky and Guildford, 1984; Venables and Moore, 2010) thresholds developed for growth rates to P–E parameters and GPP rates should be interpreted with caution with consistency among the various metrics being the strongest evidence to support a characterization of light and/or nutrient limitation.

Data analyses and statistics

All data were tested for normality with the Shapiro Wilk test ($p < 0.05$) and transformed appropriately to achieve normal distribution prior to all statistical analyses. Linear regression analyses were employed to assess the relationships ($p < 0.05$) between our proxies for phytoplankton biomass and to calibrate the sonde-derived fluorescence values. The differences in biomass, P–E parameters, and nutrient status between light deficient and sufficient samples were assessed with an Analysis of Variance (ANOVA). To test for monthly differences in the model derived (Eq. (3)) P–E parameters, we employed a Kruskal–Wallis H test ($p < 0.05$). The ϕ_{PSII} experiments were tested for significance by applying ANOVAs to triplicate measurements of the experimental treatments, and if significant, were followed with post hoc Dunnett-tests (pairwise comparison, two-sided), comparing the control treatment to + N, + P, and + N + P additions.

In order to assess spatial differences and address questions related to the reservoir continuum concept, sample sites were grouped together into 4 regions (Fig. 1). The regions were chosen to represent the three regions of reservoir dynamics: up-reservoir, riverine; down-reservoir, transitional; and the arms, lacustrine regions (Kimmel and Groeger, 1984). Physical (two light parameters), biological (five phytoplankton parameters), photosynthesis-irradiance (five parameters), and nutrient status indicator (seven parameters) data were then analyzed for regional and monthly differences with the linear mixed effect (LME) analyses of the nlme-package (statistical program R, version 3.1.0). The model was followed with an ANOVA and significant treatment effects were subjected to a post hoc interaction test with pairwise comparisons between factors using the phia-package in R. Interactions between the two factors were not applied to the nutrient status parameters impacted by high turbidity due to their smaller sample size. We used the following model structure for the majority of the parameters; for all turbidity-

impacted nutrient status parameters, a simplified version of the model was applied without the interaction term:

$$Y_i = \beta_0 + \beta_1 \text{Month} + \beta_2 \text{Region} + \beta_3 \text{Month} * \text{Region} + \text{Site} + \varepsilon_i \quad (5)$$

where Y_i was the transformed parameter Y (e.g., Chl a) at site i , while Month and Region were fixed effects representing June–October and the four regions of the reservoir, respectively. β_0 was the average dependent variable when the month and region were one. β_1 to β_3 were the average differences in the dependent variable between months when controlling for region (β_1), between regions when controlling for month (β_2), and the interactions (β_3). Site was a random effect for the sampling sites. Random effects and the residual error (ε_i) are assumed to be drawn from a normal distribution $N(0, \sigma^2)$.

Results

Mixing dynamics and light conditions

Lake Diefenbaker's maximum depth (Z_{\max}) and stability of the water column increased along the length of the reservoir (Table 3) from consistently isothermal M3 (Fig. 1; Z_{\max} of 14 m) to seasonally stratified M8 in the Gardiner arm (Fig. 1; Z_{\max} of 51 m). All sites in the lacustrine arms were stratified from June to October, with the exception of the Qu'Appelle arm in October. Relative to the Gardiner and Qu'Appelle arms, the up- and down-reservoir stations exhibited reduced water clarity as shown by shallower Secchi disk depths (Table 3) and significantly higher attenuation coefficients (K_{dPAR} ; Tables 1, 3, 4), particularly up-reservoir. This pattern of increased light penetration in the arms is consistent with the highest sediment deposition rates occurring up-reservoir (Sadeghian et al., in this issue). The attenuation of PAR was highest at up-reservoir locations (mean of 2.7 m^{-1}) and declined in the arms (mean of 0.5 m^{-1} ; Table 3), illustrating the spatial gradient in both trophic status and turbidity due to the inflowing SSR.

The mean irradiance (\bar{E}_{24}) experienced by algal cells that are evenly mixed throughout the epilimnion was used to assess light deficiency (Figs. 2A, B). We tested the assumption of an even distribution of cells in the mixed layer through an examination of the monthly Chl a

Table 3
Lake Diefenbaker limnological parameters and nutrient chemistry during the open-water season of 2013. Shown are the arithmetic mean and 95% confidence intervals (lower limit, upper limit) of n samples, numbers in superscript indicate n values that differed from those reported in the column headers. See Table 1 for parameter definitions and units. POC excludes samples subjected to high turbidity (>20 NTU).

Parameter	Up-reservoir ($n = 15$)	Down-reservoir ($n = 20$)	Gardiner arm ($n = 15$)	Qu'Appelle arm ($n = 10$)
Physical				
Z_{\max}	20.6 (17.0, 24.3)	41.7 (38.9, 44.4)	50.8 (49.4, 52.3)	29.2 (25.3, 33.0)
Z_{mix}	14.7 (12.1, 17.2)	18.3 (13.8, 22.8)	22.4 (16.1, 28.6)	16.2 (10.4, 22.0)
Secchi	0.9 (0.3, 1.4) ¹⁴	2.6 (1.8, 3.4) ¹⁸	4.6 (4.0, 5.2) ¹⁴	4.2 (3.4, 4.9)
K_{dPAR}	2.73 (1.33, 4.14) ¹⁴	1.06 (0.47, 1.65)	0.46 (0.43, 0.49) ¹⁴	0.53 (0.41, 0.65)
\bar{E}_{24}	24.1 (8.8, 39.5) ¹³	35.5 (26.1, 44.9)	55.5 (31.9, 79.2) ¹⁴	68.2 (33.7, 102.7)
Chemical				
TP	1.36 (0.67, 2.05)	0.66 (0.42, 0.90)	0.41 (0.34, 0.47)	0.42 (0.35, 0.49)
TDP	0.29 (0.17, 0.41)	0.27 (0.15, 0.38)	0.15 (0.14, 0.17)	0.16 (0.14, 0.19)
PP	0.90 (0.40, 1.40)	0.38 (0.18, 0.58)	0.18 (0.15, 0.22) ¹⁴	0.23 (0.14, 0.32)
DRP	0.19 (0.07, 0.31)	0.06 (0.04, 0.07)	0.04 (0.03, 0.05)	0.04 (0.02, 0.05)
TN	37.00 (30.03, 43.98)	51.90 (46.35, 57.44)	43.72 (40.89, 46.54)	43.37 (39.77, 46.96)
TDN	31.72 (25.01, 38.44)	46.83 (42.53, 51.11)	39.02 (36.02, 42.02)	38.29 (34.27, 42.29)
PN	8.5 (6.0, 11.0)	5.3 (3.4, 7.3)	3.8 (3.0, 4.5)	4.4 (3.6, 5.3)
NH_4^+	1.32 (0.77, 1.86)	1.01 (0.61, 1.41)	0.63 (0.45, 0.80)	0.60 (0.42, 0.78)
NO_3^-	16.96 (10.15, 23.78)	33.63 (29.84, 37.42)	27.85 (25.58, 30.12)	27.20 (24.00, 30.39)
TDFe	2.11 (0.09, 4.13)	0.83 (−0.17, 1.82) ¹⁸	0.05 (0.03, 0.07)	0.05 (0.02, 0.08)
DRSi	113.99 (99.44, 128.53) ¹⁴	107.08 (93.96, 120.20)	71.14 (58.19, 84.08)	80.08 (63.06, 97.10)
Biological				
Chl a	3.2 (1.6, 4.8)	3.5 (1.8, 5.3)	2.1 (1.7, 2.4)	2.5 (2.1, 3.0)
POC	42.1 (27.6, 56.6) ¹¹	31.3 (17.7, 44.8) ¹⁸	22.7 (18.6, 26.7) ¹⁵	29.7 (22.6, 36.9) ⁹
Phyto	268.48 (−129.29, 666.25) ⁵	226.45 (93.54, 445.16) ¹⁰	141.15 (83.64, 198.66) ⁵	NE
% cont. Crypto & Bacill	90 (83, 97) ⁵	90 (84, 96) ¹⁰	71 (43, 98) ⁵	NE

NE, phytoplankton samples from the Qu'Appelle arm were not enumerated.

Table 4

Linear mixed effect (LME) model output of physical, biological, photosynthesis-irradiance (P-E), and nutrient status indicator data. Data was tested for the effect of regional and monthly factors. An ANOVA was included in the LME analyses (F and p values) and if factors were significant, a post hoc test was conducted (as indicated by lower case letters where similar letters are not significantly different from each other; $p > 0.05$). U, up-reservoir; D, down-reservoir; G, Gardiner arm; Q, Qu'Appelle arm; Jn, June; Jl, July; A, August; S, September; O, October. In the first column, superscript ^a, includes all data while superscript ^b, excludes samples subjected to high turbidity (>20 NTU) so due to this smaller sample size interactions (region * month) were not included in the model. See Table 1 for parameter definitions and units.

		Fixed effect	F value	p value	Regional analyses				Monthly analyses				
					U	D	G	Q	Jn	Jl	A	S	O
<i>Physical</i>													
K_{dPAR}^a	Region	$F_{3,8} = 31.352$	0.0001	a	b	c	c						
	Month	$F_{4,30} = 9.465$	<0.0005					a	b	a	a	a	
	Interaction: Region * Month	$F_{12,30} = 3.762$	0.0016										
\bar{E}_{24}^a	Region	$F_{3,8} = 12.422$	0.0022	a	b	c	c						
	Month	$F_{4,29} = 10.861$	<0.0005					a	b	a	a	c	
	Interaction: Region * Month	$F_{12,29} = 4.025$	0.0011										
<i>Biological</i>													
$Chl\ a^a$	Region	$F_{3,8} = 0.542$	0.6670										
	Month	$F_{4,32} = 5.656$	0.0015					a	b	b	b	b	
	Interaction: Region * Month	$F_{12,32} = 2.789$	0.0102										
POC:Chl a^b	Region	$F_{3,8} = 1.958$	0.1990										
	Month	$F_{4,37} = 1.850$	0.1401										
Phyto ^a	Region	$F_{2,1} = 0.126$	0.8939										
	Month	$F_{4,4} = 8.866$	0.0287					a	bc	b	d	c	
	Interaction: Region * Month	$F_{8,4} = 2.235$	0.2280										
Crypto ^a	Region	$F_{2,1} = 3.516$	0.3528										
	Month	$F_{4,4} = 6.054$	0.0546										
	Interaction: Region * Month	$F_{8,4} = 2.291$	0.2206										
Bacill ^a	Region	$F_{2,1} = 5.602$	0.2863										
	Month	$F_{4,4} = 23.452$	0.0049					a	b	cf	df	e	
	Interaction: Region * Month	$F_{8,4} = 6.488$	0.0443										
<i>P-E</i>													
E_K^a	Region	$F_{3,8} = 11.361$	0.0003	a	b	c	c						
	Month	$F_{4,153} = 6.795$	<0.0005					a	b	ab	ab	c	
	Interaction: Region * Month	$F_{4,153} = 4.450$	<0.0005										
α^a	Region	$F_{3,8} = 0.998$	0.4420										
	Month	$F_{4,32} = 11.879$	<0.0005					a	b	a	ab	c	
	Interaction: Region * Month	$F_{12,32} = 2.601$	0.0154										
$rETR_{max}^a$	Region	$F_{3,8} = 5.110$	0.0290	a	b	c	bc						
	Month	$F_{4,32} = 5.754$	0.0013					a	a	a	a	b	
	Interaction: Region * Month	$F_{12,32} = 2.073$	0.0496										
ϕ_{PSII}^a	Region	$F_{3,8} = 0.554$	0.6599										
	Month	$F_{4,32} = 13.414$	<0.0005					ab	a	b	b	c	
	Interaction: Region * Month	$F_{12,32} = 1.927$	0.0687										
GPP ^a	Region	$F_{3,8} = 5.961$	0.0195	a	b	b	b						
	Month	$F_{4,32} = 2.515$	0.0608										
	Interaction: Region * Month	$F_{12,32} = 1.027$	0.4487										
<i>Nutrient status</i>													
TT ^a	Region	$F_{3,8} = 3.078$	0.0905										
	Month	$F_{4,32} = 7.856$	0.0002					a	ab	b	ab	c	
	Interaction: Region * Month	$F_{12,32} = 1.728$	0.1069										
APA ^a	Region	$F_{3,8} = 2.944$	0.0987										
	Month	$F_{4,32} = 6.412$	0.0007					a	a	b	a	b	
	Interaction: Region * Month	$F_{12,32} = 1.656$	0.1252										
N:p ^b	Region	$F_{3,8} = 6.048$	0.0187	a	b	c	c						
	Month	$F_{4,37} = 1.690$	0.1731										
P-debt ^b	Region	$F_{3,8} = 0.425$	0.7382										
	Month	$F_{4,38} = 2.831$	0.0378					a	ab	a	a	b	
C:p ^b	Region	$F_{3,8} = 4.727$	0.0351	a	a	b	b						
	Month	$F_{4,36} = 1.484$	0.2276										
N-debt ^b	Region	$F_{3,8} = 1.176$	0.3777										
	Month	$F_{4,38} = 4.806$	0.0031					ab	a	ab	b	c	
C:N ^b	Region	$F_{3,8} = 0.475$	0.7084										
	Month	$F_{4,37} = 3.358$	0.0193					a	a	b	b	ab	

fluorescence profiles as a proxy for algal biomass (Electronic Supplementary Material (ESM) Appendix S1). While the validity of this assumption fluctuated on a monthly basis in the Gardiner arm, the Chl a maxima were consistently within the mixed layer with a notable absence of deep chlorophyll maximums (DCMs; Mellard et al., 2011). As well, given the vertical diel migration of phytoplankton (Mellard et al., 2011), profiles collected during daylight hours may not be representative of algal distributions on a 24-h basis. Chl a maxima got progressively closer to the surface over the season (ESM Appendix S1) corresponding

with the decreasing \bar{E}_{24} values (Fig. 2B), providing further indications that changes in the \bar{E}_{24} values reflect the mean light environment in the reservoir.

Light deficiency was prominent in the up-reservoir section with a seasonal \bar{E}_{24} mean ($24 \mu\text{mol m}^{-2} \text{s}^{-1}$) well below the 41.7 threshold (Table 2) except for the month of September when light was sufficient (Fig. 2B). Down-reservoir \bar{E}_{24} values were variable but had greater average light than up-reservoir, with June and September being light sufficient. The arms were mostly light sufficient during the summer

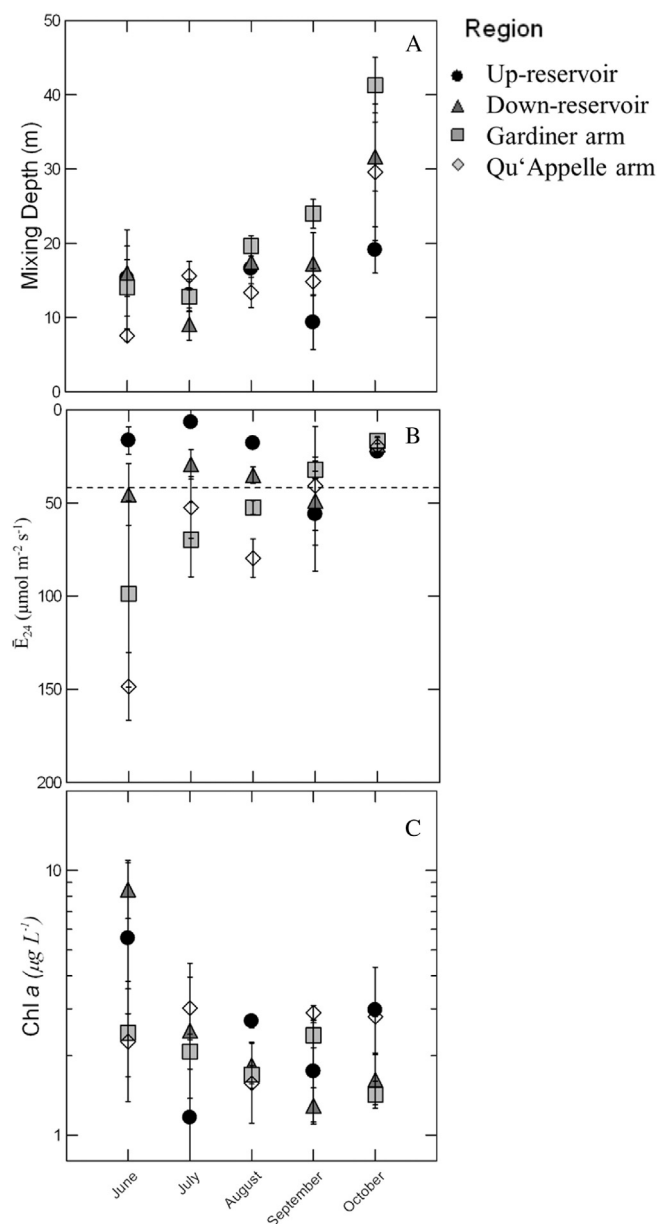


Fig. 2. Monthly and regional patterns in physical and biological parameters. Monthly means are shown with standard error bars. Panels show A) mixing depth, B) mean daily photosynthetically active radiation (\bar{E}_{24}) displayed on a reversed Y-axis, C) chlorophyll *a* (Chl *a*) concentration on a log₁₀ scale. Values above dashed lines are considered light deficient (Table 2; Hecky and Guildford, 1984).

although \bar{E}_{24} decreased in the fall because of deeper mixing depths and shorter daily incident irradiance (e.g., October \bar{E}_0 values were 1.5 times lower than in June, data not shown). This resulted in \bar{E}_{24} values for the Gardiner and Qu'Appelle arms in September and October being less than the indicator threshold and suggestive of light deficiency (Figs. 2A, B). Epilimnetic mean irradiance was significantly lower throughout the reservoir in October, relative to the other months (Table 3).

Indicators of phytoplankton biomass

Three different indicators were used to represent the in situ phytoplankton population including phytoplankton biomass via microscopic counts, Chl *a*, and POC concentrations. We found a significant positive relationship between POC and Chl *a* ($R^2_{\text{adj}} = 0.614$, $n = 53$, $p < 0.0005$) as well as between phytoplankton biomass and Chl *a* ($R^2_{\text{adj}} =$

0.639, $n = 18$, $p < 0.0005$; Fig. 3B) for samples with turbidity less than 20 NTU. There was no relationship between POC and Chl *a* with the inclusion of samples of all turbidities (Fig. 3A). Therefore, we chose not to include the 6 samples (M3, June 5; M3, M5, U1-M, C1-M, July 4; U2-M, July 16) collected during conditions of high turbidity (>20 NTU) in the reporting of our POC concentrations. These high turbidity samples were also excluded from our application of turbidity-sensitive nutrient status indicators including all stoichiometric particulate ratios and the two debt assays. These relationships, combined with the significant positive ones between particulate N, particulate P, and Chl *a* concentrations (data not shown) assured us that the particulate nutrients and Chl *a* concentrations represented phytoplankton biomass in LD and validated our use of them as nutrient status indicators.

The regulation of POC:Chl *a* intracellular stoichiometry is a universal response of phytoplankton communities to both nutrient and light limitation (Table 2, Geider et al., 1997; Healey and Hendzel, 1979b). In 2013, the mean reservoir POC:Chl *a* ratio was $11.4 \pm 4.5 \mu\text{mol C } \mu\text{g Chl } a^{-1}$, indicating that the LD phytoplankton community experienced nutrient deficiencies (Table 2), though no regional or monthly differences were detected (Table 4).

Both Chl *a* concentrations and total phytoplankton biomass showed no significant differences between regions, though monthly differences were detected (Table 4, Figs. 2C and 4). Peak biomass occurred in June, with a second much smaller peak in October (Table 4, Fig. 4). The phytoplankton community consisted mostly of cryptophytes and bacillariophytes; combined, they contributed 90% (up- and down-reservoir) to the total phytoplankton biomass (Table 3, Fig. 4). The same taxa formed a smaller proportion of the phytoplankton community in the Gardiner arm (38–89%) due to an increase in dinoflagellates and chlorophytes during July and August (Fig. 4).

There were no significant differences between light deficient and sufficient categories using the \bar{E}_{24} threshold for all three indicators of phytoplankton biomass nor the Phyto:Chl *a* ratio (Table 5). However, the POC:Chl *a* ratio was significantly lower during light deficient conditions (Table 5).

P–E parameters

The ratio of the mean mixed layer irradiance (\bar{E}_{24}) relative to the P–E parameter representing the irradiance at which the photosynthetic electron transport begins to be saturated (E_K ; Fig. 5A) is an additional indicator of light deficiency in phytoplankton communities ($\bar{E}_{24}/E_K < 1$; Table 2; Hecky and Guildford, 1984). The mean ratio in LD was consistently less than 1 (0.12 ± 0.11). Therefore, since E_K was never greater than \bar{E}_{24} (Figs. 2, 5), it indicates that the LD phytoplankton communities were exposed to a mean light climate well below light saturation as illustrated by the $rETR_{\text{max}}$ (Table 1) mean value of 257.

Upon division into light deficiency and sufficiency using the \bar{E}_{24} threshold, all of the P–E parameters (E_K , $rETR_{\text{max}}$, ϕ_{PSII} , GPP; Table 1) with the exception of the slope of the P–E curve (α), exhibited significant differences (Table 5). Significant regional and monthly differences in E_K (Table 4, Fig. 5A) reflected the gradually increasing values over the season for the down-reservoir and Gardiner arm samples, resulting in E_K maxima in October (Fig. 5A). $rETR_{\text{max}}$ peaks also occurred in October (Table 4, Fig. 5C). Both E_K and $rETR_{\text{max}}$ significantly declined during conditions of light sufficiency (Table 5).

The quantum efficiency of photosystem II (ϕ_{PSII}) was the most variable in the up-reservoir region, whereas in the down-reservoir, Gardiner and Qu'Appelle arms, values slowly increased throughout the sampling period (Fig. 5D). In October, the ϕ_{PSII} was significantly higher than all previous months (Table 4, Fig. 5D) with mean values in all regions close to the empirical maximum value of ~ 0.65 (Kolber and Falkowski, 1993). Under light sufficient conditions (according to the \bar{E}_{24} threshold), the ϕ_{PSII} values also significantly decreased (Table 5). Rates of GPP showed a significant response to improved light conditions, with a 56% increase observed (Table 5). Up-reservoir samples

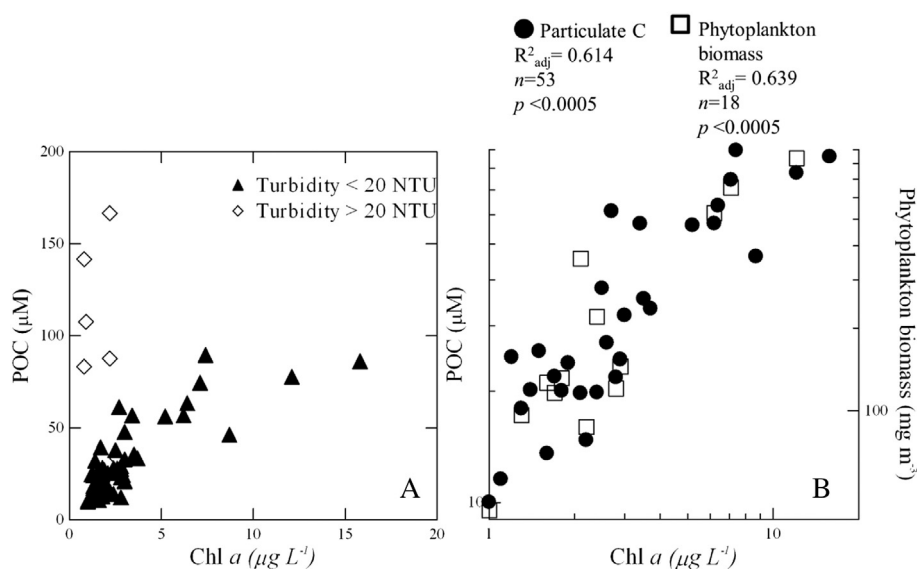


Fig. 3. Relationships between indicators of phytoplankton biomass. Panels show A) the relationship between POC and Chl *a* concentrations for the entire dataset, where samples collected during conditions of high turbidity (>20 NTU) are indicated; B) the relationship between POC, phytoplankton biomass, and Chl *a* concentrations (exclusive of the high turbidity samples). Significant positive relationships were found between POC and Chl *a* (shaded circles), and also between phytoplankton biomass and Chl *a* (open squares). Note the \log_{10} axes.

were significantly less productive than the rest of the reservoir, and no seasonal patterns were apparent (Table 4, Fig. 5E). The highest GPP rates occurred in the Gardiner arm in June (Fig. 5E).

The P–E curve derived from model fit (Eq. (3); Webb et al., 1974) to gross primary production normalized to Chl *a* (GPP^B ; Table 1) and \bar{E}_{24} for samples collected in August illustrate a positive slope (GPP^B/\bar{E}_{24}) at low irradiances ($<50.0 \mu\text{mol m}^{-2} \text{s}^{-1}$). All samples collected at in situ \bar{E}_{24} values $>40 \mu\text{mol photons m}^{-2} \text{s}^{-1}$ were P deficient as assessed by particulate N:P ratios (Fig. 6). Similar P–E curve fits were applied to all of the months sampled and an open-water mean for the reservoir was calculated (Table 6). The 95% confidence intervals for the P–E model output \bar{E}_{24} representing the inflection from the slope to the GPP^B_{max} bracket the \bar{E}_{24} threshold of $41.7 \mu\text{mol m}^{-2} \text{s}^{-1}$ for all months with the exception of October. There were no significant differences between months for either the GPP^B/\bar{E}_{24} ratio nor the \bar{E}_{24} threshold ($H_{5,4} = 4.000$, $p = 0.406$; Table 6). The open-water mean \bar{E}_{24} threshold of $35.1 \mu\text{mol m}^{-2} \text{s}^{-1}$ (Table 6) was similar to our \bar{E}_{24} breakpoint identified at $34.7 \mu\text{mol m}^{-2} \text{s}^{-1}$.

Phytoplankton community nutrient status

Based on TP concentrations, LD's regions can be categorized as meso- to eu-trophic in the up- and down-reservoir sections, and meso- to oligo-trophic in the Gardiner and Qu'Appelle arms (Table 3;

Wetzel, 2001). Phosphorus (TP, Particulate P, TDP, DRP) concentrations decreased from the inflow to the outflow (Table 3), although spatial N concentration patterns were different, and indicate in-reservoir N processing (Table 3).

The P status indicators (TT, APA, P-debt, N:P, C:P) were all in agreement, and indicated moderate to extreme P deficiency throughout the open-water season. Exceedances of the four P status indicator thresholds (Table 2) occurred 65% of the times measured, indicating P deficiency was prominent. Division of these four P status measurements into light sufficient and deficient categories revealed that P status thresholds were exceeded 90% of the times measured under conditions of light sufficiency, and only 46% of the times measured under conditions of light deficiency. According to all of the P status indicators, during conditions of light sufficiency the phytoplankton communities were significantly more P deficient than during light deficiency (Table 5). The physiological indicators (TT, APA, P-debt) all showed significant monthly declines from June until October, though no regional differences were detected (Table 4, Fig. 7). The stoichiometric indicators (N:P, C:P) agreed with each other, but showed different seasonal and spatial patterns than the physiological indicators. Although the temporal pattern of P deficiency was not apparent in the stoichiometric indicators, their regional patterns indicated that the arms were significantly more P deficient than the up- and down-reservoir regions (Table 4, Fig. 7).

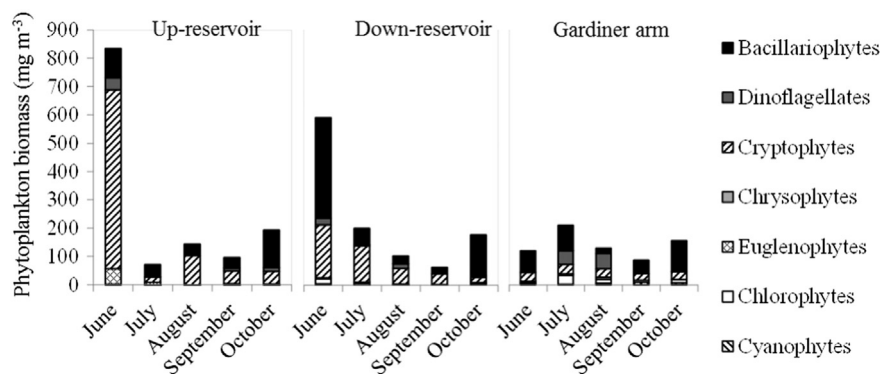


Fig. 4. Biomass of the major phytoplankton groups in 3 regions of the reservoir; up-reservoir (U1-M), down-reservoir (U2-M and C3-M), and the Gardiner arm (U3-M), during the open-water season of 2013 ($n = 20$).

Table 5
Phytoplankton biomass, photosynthetic parameters, and nutrient status indicators separated into in situ light deficient and sufficient categories. Mean and 95% confidence intervals of parameters divided into light deficient and light sufficient samples (Table 2) through the application of an indicator threshold for the mean light experienced by a freely circulating algal cell during a 24 hour period (\bar{E}_{24}) representing the balance between light deficiency ($<41.7 \mu\text{mol photons m}^{-2} \text{s}^{-1}$) and light sufficiency ($>41.7 \mu\text{mol photons m}^{-2} \text{s}^{-1}$; Table 2; Hecky and Guildford, 1984). Differences between light deficient and sufficient samples were tested using an ANOVA ($p < 0.05$). Bold values indicate nutrient deficiencies (Table 2). In the first column, superscript ^a, indicates all data included while superscript ^b, indicates samples subject to high turbidity ($>20 \text{ NTU}$) were excluded. See Table 1 for parameter definitions and units.

		Light deficient	Light sufficient
		$\bar{E}_{24} < 41.7$	$\bar{E}_{24} > 41.7$
		Mean (lower limit, upper limit)	Mean (lower limit, upper limit)
<i>Biomass</i>			
Phyto ^a	$F_{1,18} = 0.004, p = 0.953$	252.78 (102.78, 402.79)	200.45 (27.94, 372.96)
Chl <i>a</i> ^a	$F_{1,55} = 0.250, p = 0.619$	3.0 (1.9, 4.1)	2.8 (1.9, 3.6)
POC ^b	$F_{1,48} = 2.830, p = 0.099$	29.2 (20.2, 38.2)	32.6 (25.4, 39.8)
Phyto:Chl <i>a</i> ^a	$F_{1,18} = 0.096, p = 0.760$	83.1 (42.2, 124.0)	77.6 (52.5, 102.7)
POC:Chl <i>a</i> ^b	$F_{1,47} = 10.522, p = 0.002$	9.8 (8.3, 11.3)	13.7 (11.7, 15.7)
<i>P–E parameters</i>			
E_k ^a	$F_{1,55} = 24.269, p < 0.0005$	524 (480, 569)	383 (355, 410)
α ^a	$F_{1,55} = 3.043, p = 0.087$	0.56 (0.53, 0.58)	0.53 (0.51, 0.54)
rETR _{max} ^a	$F_{1,55} = 23.452, p < 0.0005$	287.6 (260.6, 314.6)	199.7 (178.8, 220.6)
Φ_{PSII} ^a	$F_{1,55} = 9.413, p = 0.003$	0.59 (0.56, 0.62)	0.53 (0.52, 0.55)
GPP ^a	$F_{1,55} = 11.908, p = 0.001$	82 (61, 104)	147 (88, 206)
<i>Nutrient status</i>			
TT ^a	$F_{1,55} = 15.852, p < 0.0005$	357 (160, 554)	17 (9, 25)
APA ^a	$F_{1,55} = 10.949, p = 0.002$	0.272 (0.147, 0.397)	0.565 (0.399, 0.731)
N:P ^b	$F_{1,48} = 4.393, p = 0.041$	17.9 (15.4, 20.4)	20.9 (18.5, 23.3)
P-debt ^b	$F_{1,48} = 5.550, p = 0.023$	0.10 (0.08, 0.12)	0.14 (0.12, 0.17)
C:P ^b	$F_{1,47} = 4.159, p = 0.047$	111.5 (93.4, 129.6)	128.3 (115.2, 141.4)
N-debt ^b	$F_{1,49} = 24.880, p < 0.0005$	0.25 (0.10, 0.39)	0.01 (0.00, 0.02)
C:N ^b	$F_{1,48} = 0.062, p = 0.805$	6.2 (5.9, 6.6)	6.3 (5.9, 6.7)

No conditions of N deficiency were observed, as assessed by the N-debt and C:N indicators from June to September (Figs. 7H, I). In October, N deficient conditions were indicated by N-debt assays at down-reservoir locations (Fig. 7H). While there were no differences in the C:N ratios between light deficient and sufficient samples, the N-debt assay indicated that N deficiency was occurring under conditions of light deficiency (Table 5). While both indicators showed no regional differences, they had contrasting seasonal patterns, with N-debt indicating increasing N deficiency from June to October, while the C:N ratios showed the opposite trend (exclusive of October; Figs. 7H, I).

There were significant increases in Φ_{PSII} relative to controls in nutrient addition photosynthetic efficiency experiments on 6 occasions, primarily during June and July (Table 7). The responses were primarily the result of the addition of + N + P and + P, indicating P deficiency in agreement with the other P deficiency indicators (Fig. 7), though there were indications of N and P co-deficiency as well (Table 7, Fig. 7). The single response to the addition of N was not supported by the in situ N status indicators (Fig. 7). Although not significant, the majority of the time, phytoplankton communities responded positively to nutrient additions, regardless of the specific nutrient or combination (+P = +2%, +N = +1.9%, +N + P = +2.8%; Fig. 7).

Discussion

We provide evidence of light and P co-limitation of the Lake Diefenbaker phytoplankton communities during the open-water season of 2013. The impact of this co-limitation is evaluated relative to monthly and spatial differences in phytoplankton biomass and gross primary productivity. The up-reservoir region was highly affected by inflow from the SSR and experienced almost constant light limitation displaying properties typical of a riverine region. Although phytoplankton biomass was highest in this region, the maximum GPP rates were measured in June in the Gardiner arm under conditions of stratification and sufficient light. Phytoplankton communities within the transitional and lacustrine regions of the reservoir experienced symptoms of P limitation, often congruent with light sufficiency.

Impact of light and nutrient status on phytoplankton biomass and gross primary production rates

The reservoir's GPP maximum was measured in the stratified arms during spring prior to the high flow event, which coincided with the highest \bar{E}_{24} values and the highest indicators of P deficiency, illustrating the importance of nutrient use efficiency in this prairie reservoir. The influence of the turbid SSR on phytoplankton production and physiology was reflected in the low GPP rates close to the inflow, particularly during episodes of high turbidity in June and July. This was also the time of the greatest phytoplankton biomass and Chl *a* concentrations, though high concentrations of phaeophytin ($9\text{--}11 \mu\text{g L}^{-1}$; data not shown) at up-reservoir and down-reservoir locations indicated the phytoplankton in those regions were not photosynthetically active. We acknowledge that high phaeophytin concentrations can also indicate high grazing rates (Wetzel, 2001); however, we are unable to test the impact of grazing in the spring in these regions, as the only LD zooplankton data available is from a station in the Qu'Appelle arm where the effects of zooplankton on phytoplankton biomass was found to be most significant in July (Vogt et al., in this issue). This spring phytoplankton peak is consistent with the PEG model of the phytoplankton spring bloom for north temperate lakes (Sommer et al., 2012) wherein physics (light and stratification) define the start and end of the phytoplankton growth season with nutrient limitation being dominant in the summer. For example, in LD when light became sufficient, algal biomass increased resulting in increased P demand and eventual P deficiency of the phytoplankton communities.

Phytoplankton photoacclimate to higher light by reducing their light harvesting pigments and by up-regulating mechanisms that divert excess energy away from the photosystems (Arrigo et al., 2010). If photoacclimation was occurring in LD we would expect to see higher ratios of Phyto:Chl *a* and POC:Chl *a* in light sufficient relative to light deficient conditions. We do find some evidence of this, wherein the POC:Chl *a* ratio was significantly higher under light sufficient conditions. The significant positive relationship between GPP and Chl *a* concentrations ($n = 60, R^2_{\text{adj}} = 0.336, p < 0.0005$) in LD indicates moderate coupling between gross primary production and

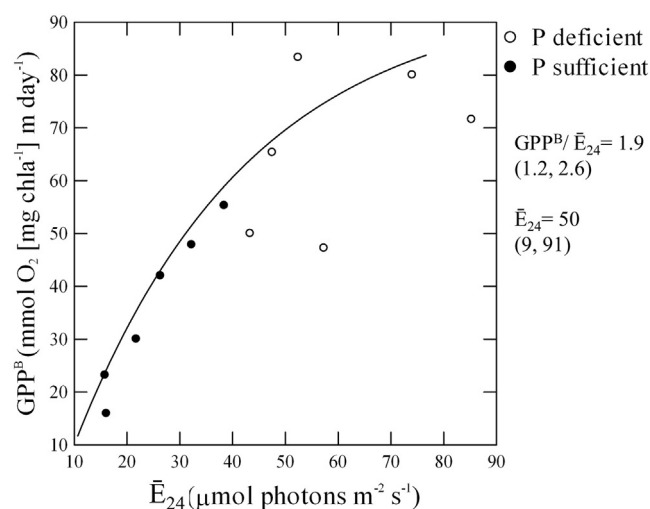
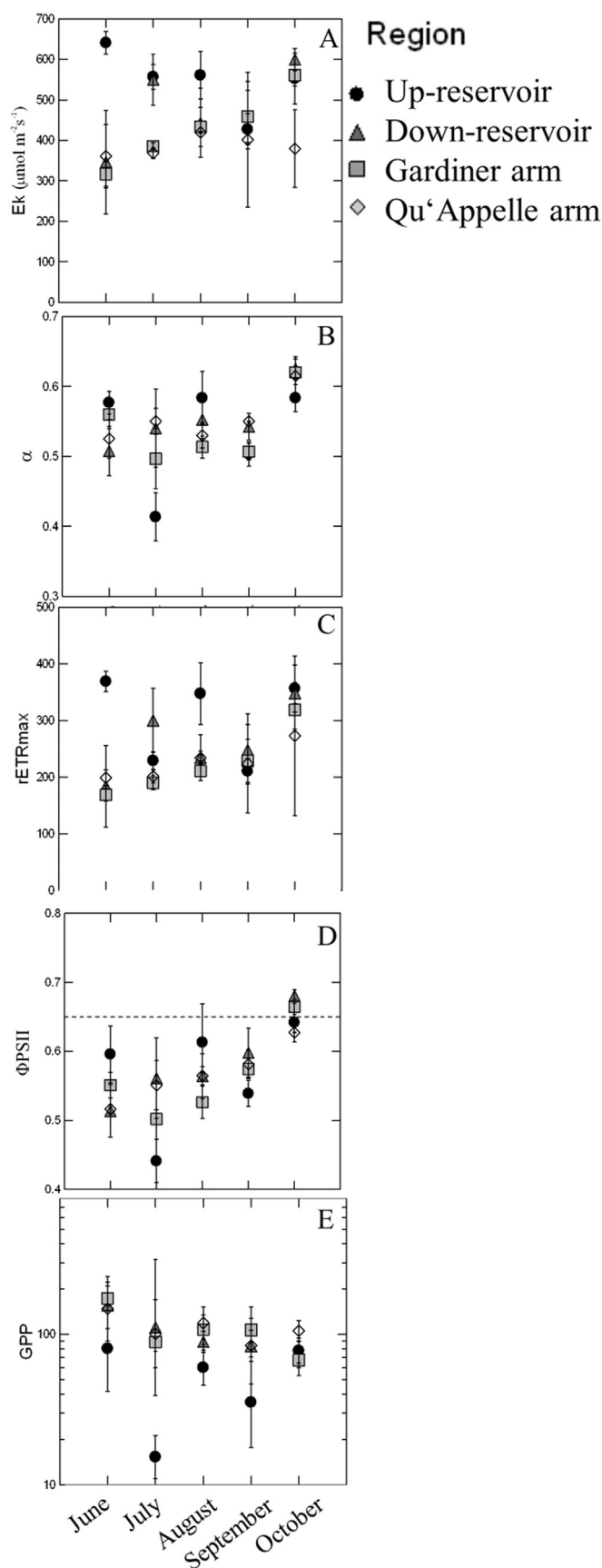


Fig. 6. P-E curve fit to gross primary production (GPP) and in situ mean daily photosynthetically active radiation (\bar{E}_{24}) illustrating light and nutrient co-limitation. Data is from 12 stations in Lake Diefenbaker sampled in August of 2013. GPP rates were derived from active fluorescence and phytoplankton absorption coefficient measurements (see [Methods](#)) and normalized to Chl *a* (denoted with the superscript B) and shown as specific rates of photosynthesis. \bar{E}_{24} values were calculated as a function of K_{dPAR} and mixed layer depth (see [Methods](#)). Model (Eq. (3)) output and associated 95% confidence intervals are given. Phosphorus status of the in situ phytoplankton communities is represented by particulate N:P ratios where values exceeding 22 (molar ratio; [Table 2](#)) are considered P deficient (open circles), while ratios less than 22 are considered P sufficient (solid circles).

light harvesting capacity in this reservoir. As expected, our active fluorescence-based measurements of GPP represent PSII reduction rates that are dependent upon how much light is absorbed and how efficiently it is processed by PSII ([Silsbe et al., 2015](#)). Within the reservoir, GPP rates increased significantly (almost doubled) at sites with higher light conditions, which was also supported by the significant changes in P-E parameters, demonstrating their ability to adjust photosynthetic capacity in response to changes in light. While light use efficiency is clearly important in LD, our data illustrate that sufficient supply of both light and P are needed to elicit positive growth and GPP rates.

Biomass accrual and photosynthetic activity are reliant upon both light and nutrients over the range of natural conditions. Phytoplankton community response to changes in light and nutrients is variable and species-specific. For example, light responses are dependent upon mobility and sinking rates, while response to nutrients are dependent on the specific cell needs such as bacillariophyte's silica requirements. This highlights the importance of using multiple lines of evidence (nutrient and light status indicators) when predicting primary producer response to environmental changes, an important consideration in managing lake and reservoir water quality.

Our GPP estimates are the first-ever reported for the whole of Lake Diefenbaker. A recent study conducted in the Qu'Appelle arm of the reservoir used alternative methods to determine net primary production (NPP) rates ([Quiñones-Rivera et al., in this issue](#)). Assuming a euphotic depth ($2 \times \text{Secchi}$) of ~ 9 m and a photosynthetic quotient of 1 ([Quiñones-Rivera et al., in this issue](#)), their mean NPP rate between May and August 2013 was $4.4 \pm 5.4 \text{ mmol O}_2 \text{ m}^{-2} \text{ day}^{-1}$ ([Quiñones-Rivera et al., in this issue](#)). Our mean June–August 2013 GPP rate for the Qu'Appelle arm ($n = 6$) was $126 \pm 37 \text{ mmol O}_2 \text{ m}^{-2} \text{ day}^{-1}$. Explanations for our considerably higher estimates could include the fact that respiration rates are not accounted for in our GPP estimates, although respiration

Fig. 5. Monthly and regional patterns in P-E parameters. Monthly means are shown with standard error bars. Panels show A) light saturation parameter (E_k), B) light limited slope of the P-E curve (α), C) maximum relative electron transport rate through PSII ($rETR_{max}$), D) maximum quantum yield of PSII (Φ_{PSII}) with the empirical maximum value of ~ 0.65 ([Kolber and Falkowski, 1993](#)) depicted with a dashed line, E) Gross primary production (GPP).

Table 6

Monthly mean and 95% confidence intervals (in parentheses) of P–E parameters derived from model fits (Eq. (3); Webb et al., 1974) to gross primary production normalized to Chl *a* (GPP^B) and in situ mean daily photosynthetically active radiation (\bar{E}_{24}) in Lake Diefenbaker in 2013. An example of the P–E curve resulting from this approach is illustrated in Fig. 6 for the month of August. The P–E model output is reported as the slope of the curve (GPP^B / \bar{E}_{24}) and an irradiance (\bar{E}_{24}) threshold that represents the inflection from the slope to the GPP^B_{max} . There were no significant monthly differences between GPP^B / \bar{E}_{24} nor the \bar{E}_{24} threshold.

Month	GPP^B / \bar{E}_{24}	\bar{E}_{24} threshold
June	1.28 (0.18, 2.38)	51.4 (–12.69, 115.49)
July	3.03 (–0.38, 6.44)	17.3 (–7.20, 41.80)
August	1.92 (1.19, 2.64)	50.0 (9.23, 90.77)
September	1.60 (0.54, 2.66)	55.5 (–23.68, 134.68)
October	3.20 (–9.91, 16.31)	1.3 (–3.99, 6.59)
Open-water mean	2.21 (1.13, 3.28)	35.1 (4.92, 65.28)

rates were reported to be low in 2013 ($P:R > 1$; Quiñones-Rivera et al., in this issue). Our GPP rates were derived from RLCs employing a range of irradiances representing in situ light conditions ($3\text{--}1461 \mu\text{mol photon m}^{-2} \text{s}^{-1}$), while their rates were derived from bottles incubated under constant illumination ($450 \mu\text{mol photon m}^{-2} \text{s}^{-1}$; Quiñones-Rivera et al., in this issue), which could also explain the large differences in our estimates. In comparison with other large lakes and reservoirs, Lake Diefenbaker GPP rates ($108.2 \pm 100.6 \text{ mmol O}_2 \text{ m}^{-2} \text{ day}^{-1}$) are comparable to those measured at an oligo- meso-trophic nearshore site on Lake Ontario ($111.8 \text{ mmol O}_2 \text{ m}^{-2} \text{ day}^{-1}$; Bocaniov and Smith, 2009).

Photosynthetic efficiency responses

Active fluorescence techniques are increasingly applied to freshwater ecosystems (Guildford et al., 2013; Havens et al., 2012; Silsbe et al., 2012), enabling the non-invasive assessment of photosynthetic efficiency of in situ phytoplankton communities. As defined for LD, under light deficient conditions the phytoplankton communities responded by increasing their efficiency of light utilization resulting in significantly higher P–E parameters. In addition to light, nutrient deficiencies (Beardall et al., 2001; Geider and La Roche, 1994; La Roche et al., 1993) and phytoplankton community composition (Arrigo et al., 2010; Juneau and Harrison, 2005; Suggett et al., 2009) have been shown to influence primary photochemistry. In LD, we observed very little change in the phytoplankton community composition at the up-reservoir and down-reservoir locations. The largest seasonal change in the phytoplankton community occurred in the Gardiner arm, but was unrelated to the seasonal changes in ϕ_{PSII} . Thus, we feel it is unlikely that phytoplankton community changes had a large influence on photosynthetic efficiency during the course of our study.

When are nutrients important?

In 2013, phosphorus was the limiting nutrient in Lake Diefenbaker, just as it has been described historically (1984–1985; SEPS and EC, 1988). The one indication of N deficiency, combined with the high concentrations of dissolved iron and silica in the reservoir provide further evidence that P is the limiting nutrient. Both short-term physiological assays and long-term compositional nutrient status indicators (Davies et al., 2010; Geider and La Roche, 1994; La Roche et al., 1993) were in agreement, providing weight of evidence for P limitation of LD phytoplankton communities. We acknowledge that 2013 may not have been a representative year due to the high flow event (Hudson and Vandergucht, in this issue) which clearly influenced both the light and nutrient dynamics. For example, the mean annual external TP loading to LD for the hydrologic years 2011 and 2012 (May–April) was $1075 \text{ tonnes yr}^{-1}$; during our study period (May–October 2013) the external TP loading was 4834 tonnes (North et al., in this issue). However, because the majority of this TP load is in particulate form (Johansson

et al., 2013) and may not be biologically available, symptoms of P deficiency were still detected in the phytoplankton communities. Additional studies in this issue also provide supporting evidence of P limitation of LD phytoplankton on both decadal (1995–2013; Vogt et al., in this issue) and multi-year (2010–2013; Quiñones-Rivera et al., in this issue) scales, illustrating that the high P loading in 2013 did not substantially modify phytoplankton community response to P within the reservoir.

Co-limitation of light and nutrients has been documented for algal batch cultures (Healey, 1985; Rhee and Gotham, 1981). Healey (1985) noted that at low light, there was a greater increase in N requirement relative to that for P, which may explain why our N-debt assays indicated increased uptake under light deficient conditions, while our P indicators showed the opposite response. These opposing responses can also be explained by the mechanisms causing the light deficient conditions in the reservoir. The high N-debts occurred in the dimictic down-reservoir and Gardiner arm regions during the month of October where light deficiency was induced by deeper mixing depths and shorter daily incident irradiance. These deeper mixing depths reflect the erosion of the thermocline in October, which combined with the P sufficiency of the phytoplankton community as assessed by P status indicators, suggests that P internally loaded from sediments may have become available to the pelagic phytoplankton during fall overturn. Evidence supporting this can be found in a companion study (North et al., in this issue), wherein bottom water DRP concentrations exhibited a seasonal maximum during the isothermal fall period in the arms, indicating a new supply of P through internal P loading from sediments. We suggest that the higher N deficiency in the fall was due to a combination of light deficient conditions and a pulse of biologically available P from the bottom waters.

Year-round internal P loading rates within the reservoir only represent ~24% of the annual external TP load (North et al., in this issue). The temporal coherence of internal P loading and maximum GPP and biomass peaks are offset in LD. This temporal disconnect wherein a new source of P is available to phytoplankton during light deficient conditions may explain why algal blooms are infrequent in LD (Yip et al., in this issue). However, internal P loading may be more influential in the Qu'Appelle arm which is unique from the rest of the reservoir due to its polymictic and quiescent nature (Hudson and Vandergucht, in this issue), highest rates of internal P loading (North et al., in this issue), and the highest \bar{E}_{24} values in the reservoir. Yip et al. (in this issue) identified 12 historical algal bloom events since 1984 (defined as $>8 \mu\text{g chl L}^{-1}$) through analyses of satellite images of LD; 100% of the blooms occurred in the Qu'Appelle arm. Here, the synchronization of light and nutrient supply may be supporting these blooms.

Support for the reservoir continuum concept

The reservoir continuum concept states that within the riverine zone, high, particulate (largely mineral) turbidity reduces light penetration and limits primary production (Kimmel and Groeger, 1984). The up-reservoir region of LD fits this description, as it has the poorest light conditions (highest K_{dPAR} and lowest \bar{E}_{24}), with light deficiency detected 85% of the times measured in 2013. The lowest GPP rates were also measured in this region indicating light limitation, and the higher ratio of non-algal:algal optical constituents should also be considered. Within the transition zone, which is responsive to changes in the flow regime, decreased turbidity results in enhanced depth of light penetration and increased rates of primary productivity (Kimmel and Groeger, 1984). Due to the high flow event of 2013, it is likely that our down-reservoir stations experienced a poorer light environment than expected in a year with lower flows, as the phytoplankton communities were still light limited 75% of the time in the down-reservoir region. However, GPP was responsive to higher \bar{E}_{24} values, with higher rates in the down-reservoir and arm regions. The lacustrine zone is typically an environment where phytoplankton communities are limited by nutrients (Kimmel and Groeger, 1984). Support for this has been reported in

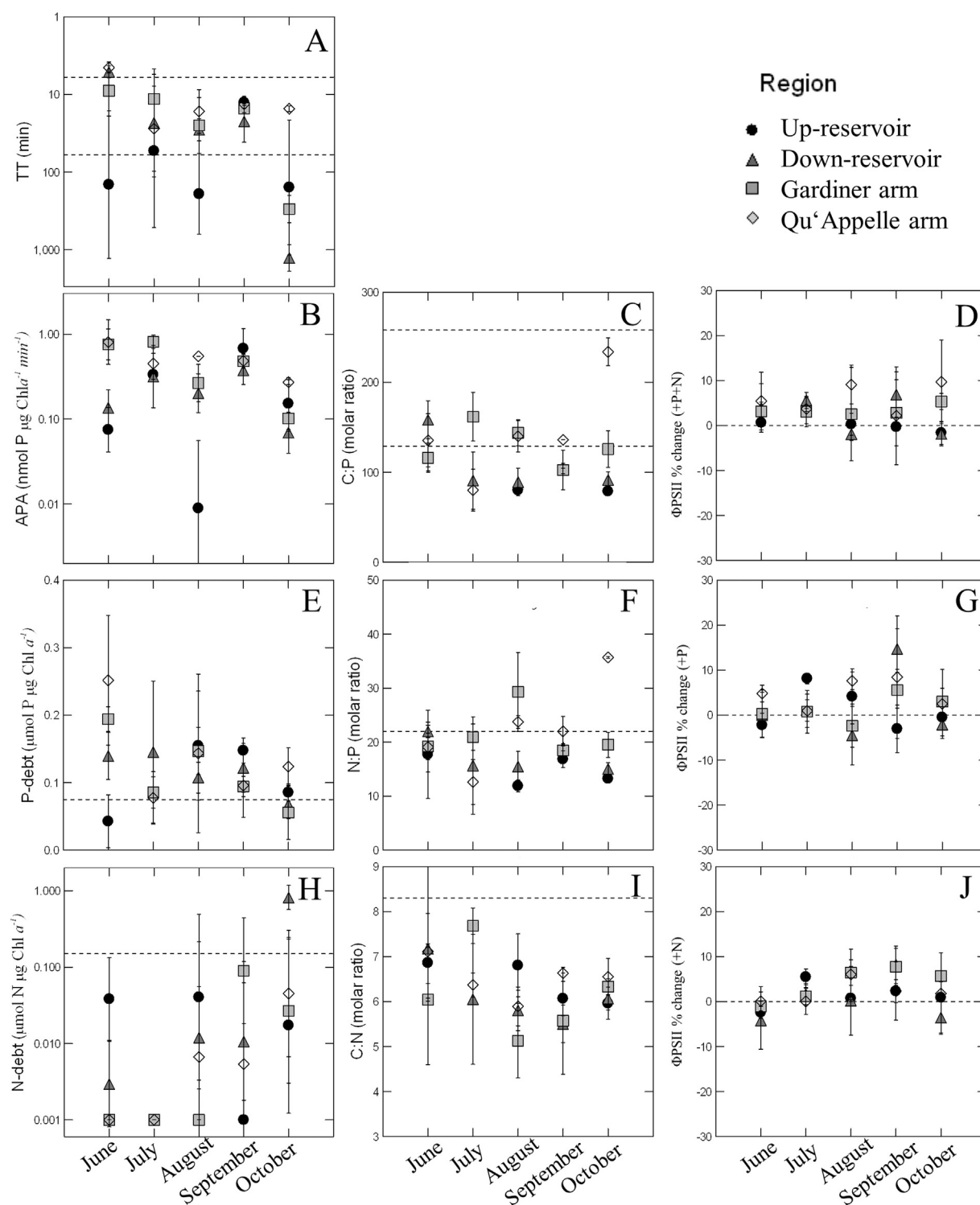


Fig. 7. Monthly and regional patterns in nutrient status indicators. Monthly means are shown with standard error bars. Panels A–C and E–G are indicators of P deficiency, panels H–J are indicators of N deficiency and panel D represents P and N co-deficiency derived from photosynthetic efficiency experiments. Panels show A) turnover time of phosphate (TT) on a reversed log₁₀ Y-axis, B) alkaline phosphatase activity (APA) displayed on a log₁₀ Y-axis, C) particulate carbon to particulate P (C:P) ratio, excluding highly turbid samples, D) percent change in Φ_{PSII} relative to a control after the addition of both P and N, E) P-debt, excluding highly turbid samples, F) particulate nitrogen to particulate phosphorus (N:P) ratio, excluding highly turbid samples, G) percent change in Φ_{PSII} relative to a control after the addition of P, H) N-debt, excluding highly turbid samples, I) particulate C to particulate N (C:N) ratio, excluding highly turbid samples, J) percent change in Φ_{PSII} relative to a control after the addition of N. Values above dashed lines indicate cases of nutrient deficiency (Table 2) and in case of the top-most dashed line in A and C, extreme deficiency.

Tennessee reservoirs, wherein APA increased from riverine to lacustrine regions (Elser and Kimmel, 1985). While this was not supported by our physiological indicators, evidence of higher P limitation in the lacustrine regions was found in our compositional indicators, which were in agreement with the longitudinal P chemistry gradients. Given that the

LD phytoplankton communities still experienced light limitation 36 and 30% of the time in the Gardiner and Qu'Appelle arms respectively, we believe the compositional parameters are better able to distinguish light from nutrient limitation, as has been suggested in culture studies (Healey, 1985).

Table 7

One-way ANOVA and two-sided Dunnett post hoc comparison of ϕ_{PSII} after 24 hour incubation, comparing measurements of an untreated control with samples which received additional nutrients (+P, +N, +N + P). Post hoc tests were conducted on treatments with a significant positive response to added nutrients relative to the control ($p < 0.05$ given in table).

Month	Region	Site		Post hoc test (p value)		
				P	N	NP
June	Down-reservoir	C3-M	$F_{3,8} = 7.692, p = 0.010$	0.033	0.042	0.004
		Gardiner arm	$F_{3,8} = 7.082, p = 0.012$	0.011		
		Qu'Appelle arm	$F_{3,8} = 9.029, p = 0.006$			0.003
July	Up-reservoir	M3	$F_{3,8} = 5.658, p = 0.022$	0.013		
		M5	$F_{3,8} = 6.881, p = 0.013$	0.007		0.023
October	Qu'Appelle arm	M9	$F_{3,8} = 8.976, p = 0.006$			0.002

Conclusions

Light and limiting nutrient supply need to be synchronized in order to see substantial increases in phytoplankton biomass and GPP rates. Therefore, lakes and reservoirs should not be managed explicitly for nutrients; light should be an important factor also considered. For example, Lake Champlain is globally known for its toxic algal blooms (Smeltzer et al., 2012), and has very similar open-water TP concentrations ($\sim 0.65 \mu\text{mol L}^{-1}$; Smeltzer et al., 2012) as Lake Diefenbaker ($0.71 \mu\text{mol L}^{-1}$); however, there has been a general trend of increasing Secchi disk depths over the past four decades, which are currently much deeper ($\sim 5 \text{ m}$; Smeltzer et al., 2012) than Lake Diefenbaker (3 m; Table 3). This example highlights the need to be cognizant of factors affecting the underwater light environment, as was the case involving filter-feeding dreissenid mussels in Lake Champlain. In LD, physical and biological factors influencing light include SSR flow and the composition of particulate matter and suspended sediments within it, changes in wind patterns, stratification regime and mixing dynamics, and reservoir residence times. Improvements in light conditions related to SSR flow are predicted, based on climate change projections of reduced flow (which carries the majority of the particulate load; Tanzeeba and Gan, 2012), resulting in a decline in inorganic turbidity, as also speculated by Vogt et al. (in this issue). As well, efforts to reduce particulate loads from agricultural lands upstream could have an additive effect of changing the light environment, in addition to potentially increasing bioavailable nutrient concentrations as evidenced in the Lake Erie watershed (Joosse and Baker, 2011).

This comprehensive examination of the complex interactions among light, turbidity, and nutrients in a large prairie reservoir support the light:nutrient ratio hypothesis in lakes (Sterner et al., 1997). We identified and isolated the various mechanisms affecting these limiting factors and their interactions. We also demonstrated the implications for gross primary productivity and biomass accrual, making this study a novel contribution to the literature.

Acknowledgments

This research was generously funded from grants to J.H. from the Global Institute of Water Security (GIWS), the Saskatchewan Water Security Agency (WSA-2014A-0001), and the National Sciences and Engineering Research Council (NSERC; RGPIN-250060-20). We would like to thank Nicole Michel for her statistical advice, and further acknowledge the team of the limnology laboratory at the University of Saskatchewan for their assistance in sample acquisition and processing: J. Hopkins, C. Crawford, M. Pomedli, L. Johnson, L. Haines, T. Belosowsky, H. Yip, C. Hewlett, and Y. Ponomarenko. We acknowledge the Department of Biology and Large Lakes Observatory at the University of Minnesota Duluth for their generous loan of the Water-PAM fluorometer. Guest Editor John-Mark Davies and three anonymous reviewers contributed greatly to the final version of this manuscript.

Appendix A. Supplementary data

Supplementary data to this article can be found online at <http://dx.doi.org/10.1016/j.jglr.2015.10.001>.

References

- Abirhire, O., Hunter, K., Prestie, C., Yip, H., Johansson, J., Sereda, J., North, R., Hudson, J., 2015. Influence of agriculture, urban and aquaculture land use on phytoplankton community composition in Lake Diefenbaker, SK, Canada. *J. Great Lakes Res.* (in this issue).
- American Public Health Association (APHA), 1989. *Standard Methods for the Examination of Water and Wastewater*. 16th ed. (Washington, D.C.).
- Arrigo, K.R., Mills, M.M., Kropuenske, L.R., van Dijken, G.L., Alderkamp, A.C., Robinson, D.H., 2010. Photophysiology in two major Southern Ocean taxa: photosynthesis and growth of *Phaeocystis antarctica* and *Fragilaria cylindrus* under different irradiance levels. *Integr. Comp. Biol.* 50 (6), 950–966.
- Bachmann, R.W., Canfield, D.E., 1996. Use of an alternative method for monitoring total nitrogen concentrations in Florida lakes. *Hydrobiologia* 323 (1), 1–8.
- Beardall, J., Young, E., Roberts, S., 2001. Approaches for determining phytoplankton nutrient limitation. *Aquat. Sci.* 63, 44–69.
- Belling, E.G., Sigeo, D.C., 2010. *Freshwater Algae: Identification and Use as Bioindicators*. John Wiley and Sons, UK.
- Bergmann, M., Peters, R.H., 1980. A simple reflectance method for the measurement of particulate pigment in lake water and its application to phosphorus–chlorophyll–seston relationships. *Can. J. Fish. Aquat. Sci.* 37, 111–114.
- Blackman, F.F., 1905. Optima and limiting factors. *Ann. Bot.* 19, 281–295.
- Bocaniov, S.A., Smith, R.E.H., 2009. Plankton metabolic balance at the margins of very large lakes: temporal variability and evidence for dominance of autochthonous processes. *Freshw. Biol.* 54, 345–362.
- Brodie, C.R., Leng, M.J., Casford, J.S.L., Kendrick, C.P., Lloyd, J.M., Zong, Y.Q., Bird, M.L., 2011. Evidence for bias in C and N concentrations and $\delta^{13}\text{C}$ composition of terrestrial and aquatic organic materials due to pre-analysis acid preparation methods. *Chem. Geol.* 282 (3–4), 67–83.
- Conley, D.J., Paerl, H.W., Howarth, R.W., Boesch, D.F., Seitzinger, S.P., Havens, K.E., Lancelot, C., Likens, G.E., 2009. Controlling eutrophication: nitrogen and phosphorus. *Science* 323 (5917), 1014–1015.
- Crumpton, W., Isenhardt, T., Mitchell, P., 1992. Nitrate and organic N analyses with second-derivative spectroscopy. *Limnol. Oceanogr.* 37 (4), 907–913.
- Currie, D.J., Kalf, J., 1984. A comparison of the abilities of freshwater algae and bacteria to acquire and retain phosphorus. *Limnol. Oceanogr.* 29 (2), 298–310.
- Davies, J.M., Nowlin, W.H., Mazumder, A., 2004. Temporal changes in nitrogen and phosphorus co-deficiency of plankton in lakes of coastal and interior British Columbia. *Can. J. Fish. Aquat. Sci.* 61, 1538–1551.
- Davies, J.M., Nowlin, W.H., Matthews, B., Mazumder, A., 2010. Temporal discontinuity of nutrient limitation in plankton communities. *Aquat. Sci.* 72 (4), 393–402.
- Donald, D.B., Parker, B.R., Davies, J.M., Leavitt, P.R., 2015. Nutrient sequestration in the Lake Winnipeg watershed. *J. Great Lakes Res.* 41 (2), 630–642.
- Elser, J.J., Kimmel, B.L., 1985. Nutrient availability for phytoplankton production in a multiple-impoundment series. *Can. J. Fish. Aquat. Sci.* 42, 1359–1370.
- Falkowski, P.G., Raven, J.A., 2007. *Aquatic Photosynthesis*. Princeton University Press, Princeton, New Jersey.
- Fee, E.J., 1990. Computer programs for calculating in-situ phytoplankton photosynthesis. *Can. Tech. Rep. Fish. Aquat. Sci.* No. 1740.
- Geider, R., La Roche, J., 1994. The role of iron in phytoplankton photosynthesis, and the potential for iron-limitation of primary productivity in the sea. *Photosynth. Res.* 39, 275–301.
- Geider, R., MacIntyre, H.L., Kana, T.M., 1997. Dynamic model of phytoplankton growth and acclimation: Responses of the balanced growth rate and the chlorophyll *a*: carbon ratio to light, nutrient-limitation and temperature. *Mar. Ecol. Prog. Ser.* 148, 187–200.
- Gosselain, V., Hamilton, P.B., 2000. Revisions to a key-based computerized counting program for free-living, attached, and benthic algae. *Hydrobiologia* 438, 139–142.
- Guildford, S.J., Hecky, R.E., 2000. Total nitrogen, total phosphorus and nutrient limitation in lakes and oceans: is there a common relationship? *Limnol. Oceanogr.* 45 (6), 1213–1223.
- Guildford, S.J., Bootsma, H.A., Fee, E.J., Hecky, R.E., Patterson, G., 2000. Phytoplankton nutrient status and mean water column light intensity in Lakes Malawi and Superior. *Aquat. Ecosyst. Health* 3, 35–45.
- Guildford, S.J., Hecky, R.E., Taylor, W.D., Mugidde, R., Bootsma, H.A., 2003. Nutrient enrichment experiments in tropical Great Lakes Malawi/Nyasa and Victoria. *J. Great Lakes Res.* 29, 89–106.
- Guildford, S.J., Hecky, R.E., Smith, E.H., Taylor, W.D., Charlton, M.N., Barlow-Busch, L., North, R.L., 2005. Phytoplankton nutrient status in Lake Erie 1997. *J. Great Lakes Res.* 31, 72–88.
- Guildford, S.J., Depew, D.C., Ozersky, T., Hecky, R.E., Smith, R.E.H., 2013. Nearshore-offshore differences in planktonic chlorophyll and phytoplankton nutrient status after dreissenid establishment in a large shallow lake. *Inland Waters* 3 (2), 253–268.
- Havens, S.M., Hassler, C.S., North, R.L., Guildford, S.J., Silsbe, G., Wilhelm, S.W., Twiss, M.R., 2012. Iron plays a role in nitrate drawdown by phytoplankton in Lake Erie surface waters as observed in lake-wide assessments. *Can. J. Fish. Aquat. Sci.* 69 (2), 369–381.
- Healey, F.P., 1975. Physiological indicators of nutrient deficiency in algae. *Fish. Mar. Serv. Tech. Rep. No.* 585.

- Healey, F.P., 1977. Ammonium and urea uptake by some freshwater algae. *Can. J. Bot.* 55, 61–69.
- Healey, F.P., 1985. Interacting effects of light and nutrient limitation on the growth-rate of *Synechococcus-linearis* (Cyanophyceae). *J. Phycol.* 21 (1), 134–146.
- Healey, F.P., Hendzel, L.L., 1979a. Fluorometric measurement of alkaline phosphatase activity in algae. *Freshw. Biol.* 9, 429–439.
- Healey, F.P., Hendzel, L.L., 1979b. Indicators of phosphorus and nitrogen deficiency in five algae in culture. *Can. J. Fish. Aquat. Sci.* 36, 1364–1369.
- Hecky, R.E., Guildford, S.J., 1984. Primary productivity of Southern Indian Lake before, during, and after impoundment and Churchill River diversion. *Can. J. Fish. Aquat. Sci.* 41 (4), 591–604.
- Hecky, R.E., Kilham, P., 1988. Nutrient limitation of phytoplankton in freshwater and marine environments: A review of recent evidence on the effects of enrichment. *Limnol. Oceanogr.* 33, 796–822.
- Holmes, R.M., Aminot, A., Kérouel, R., Hooker, B.A., Peterson, B.J., 1999. A simple and precise method for measuring ammonium in marine and freshwater ecosystems. *Can. J. Fish. Aquat. Sci.* 56 (10), 1801–1808.
- Hudson, J., Vandergucht, D., 2015. Spatial and temporal patterns in physical and chemical properties in a large prairie reservoir during high seasonal flows (Lake Diefenbaker, Canada). *J. Great Lakes Res.* (in this issue).
- Johansson, J., Vandergucht, D., Hudson, J., 2013. Lake Diefenbaker Water Quality Sampling Progress Report (April 2012–March 2013). Saskatchewan Water Security Agency, Saskatoon, SK.
- John, D.M., Whitton, B.A., Brook, A.J., 2002. The Freshwater Algal Flora Of The British Isles: An Identification Guide To Freshwater And Terrestrial Algae. Cambridge University Press, UK.
- Joose, P.J., Baker, D.B., 2011. Context for re-evaluating agricultural source phosphorus loadings to the Great Lakes. *Can. J. Soil Sci.* 91 (3), 317–327.
- Juneau, P., Harrison, P.J., 2005. Comparison by PAM fluorometry of photosynthetic activity of nine marine phytoplankton grown under identical conditions. *J. Photochem. Photobiol.* 81 (3), 649–653.
- Kalff, J., 2002. *Limnology: Inland Water Ecosystems*. Prentice Hall, Upper Saddle River, N.J.
- Kimmel, B.L., Groeger, A.W., 1984. Factors controlling primary production in lakes and reservoirs: a perspective. *Lake Reservoir Manage.* 1, 277–281.
- Kirk, J.T.O., 1994. *Light And Photosynthesis In Aquatic Ecosystems*. Oxford University Press, Oxford, UK.
- Kolber, Z., Falkowski, P.G., 1993. Use of active fluorescence to estimate phytoplankton photosynthesis in situ. *Limnol. Oceanogr.* 38 (8), 1646–1665.
- La Roche, J., Geider, R.J., Graziano, L.M., Murray, H., Lewis, K., 1993. Induction of specific proteins in eukaryotic algae grown under iron-, phosphorus-, or nitrogen-deficient conditions. *J. Phycol.* 29, 767–777.
- Lean, D.R.S., Abbott, A.P., Charlton, M.N., Rao, S.S., 1983. Seasonal phosphate demand for Lake Erie phytoplankton. *J. Great Lakes Res.* 9, 83–91.
- Lehner, B., Liemann, C.R., Revenga, C., Vorosmarty, C., Fekete, B., Crouzet, P., Doll, P., Endejan, M., Frenken, K., Magome, J., Nilsson, C., Robertson, J.C., Rodel, R., Sindorf, N., Wissler, D., 2011. High-resolution mapping of the world's reservoirs and dams for sustainable river-flow management. *Front. Ecol. Environ.* 9 (9), 494–502.
- Mellard, J.P., Yoshiyama, K., Litchman, E., Klausmeier, C.A., 2011. The vertical distribution of phytoplankton in stratified water columns. *J. Theor. Biol.* 269 (1), 16–30.
- Menzel, D.W., Corwin, N., 1965. The measurement of total phosphorus in seawater based on the liberation of organically bound fractions by persulfate oxidation. *Limnol. Oceanogr.* 10, 280–282.
- Muggeo, V.M.R., 2008. Segmented: an R package to fit regression models with broken-line relationships. *R News* 8 (1), 20–25.
- North, R.L., Guildford, S.J., Smith, R.E.H., Twiss, M.R., Kling, H.J., 2008. Nitrogen, phosphorus, and iron colimitation of phytoplankton communities in the nearshore and off-shore regions of the African Great Lakes. *Verh. Internat. Verein. Limnol.* 30 (2), 259–264.
- North, R.L., Johansson, J., Vandergucht, D.M., Doig, L., Liber, K., Lindenschmidt, K., Baulch, H., Hudson, J., 2015. Evidence for internal phosphorus loading in a large prairie reservoir (Lake Diefenbaker, SK). *J. Great Lakes Res.* (in this issue).
- Nusch, E.A., 1980. Comparison of different methods for chlorophyll and phaeopigment determination. *Arch. Hydrobiol. Beih. Ergebn. Limnol.* 14, 14–36.
- Parsons, T.R., Maita, Y., Lalli, C.M., 1984. *A Manual Of Chemical And Biological Methods For Seawater Analysis*. Pergamon Press, Oxford, New York.
- Quiñones-Rivera, Z.J., Finlay, K., Vogt, R.J., Leavitt, P.R., Wissel, B., 2015. Hydrologic, metabolic and chemical regulation of water-column metabolism and atmospheric CO₂ exchange in a large continental reservoir. *J. Great Lakes Res.* <http://dx.doi.org/10.1016/j.jglr.2015.05.005> (in this issue).
- Reynolds, C.S., Davies, P.S., 2001. Sources and bioavailability of phosphorus fractions in freshwaters: a British perspective. *Biol. Rev.* 76 (1), 27–64.
- Rhee, G.Y., Gotham, I.J., 1981. The effect of environmental factors on phytoplankton growth: light and the interactions of light with nitrate limitation. *Limnol. Oceanogr.* 26 (4), 649–659.
- Sadeghian, A., de Boer, D., Hudson, J., Wheeler, H., Lindenschmidt, K.-E., 2015. Lake Diefenbaker temperature and mixing model. *J. Great Lakes Res.* (in this issue).
- Saskatchewan Environment and Public Safety, Water Quality Branch and Environment Canada, Inland Waters Directorate, Water Quality Branch, 1988. Lake Diefenbaker And Upper South Saskatchewan River: Water Quality Study 1984–85. Saskatchewan Environment and Public Safety, Regina, SK (<http://library2.usask.ca/gp/sk/en/scanned/lake.diefenbaker.water.study.1988.pdf>).
- Saskatchewan Property Management Corporation (SPMC), S.D. ca, 1986. Lake Diefenbaker Depth Sounding Chart (Regina, SK).
- Saskatchewan Water Security Agency (WSWA), 2012. State of Lake Diefenbaker. Prepared for Consultation Meeting on May 30, 2012 (revised on October 19, 2012).
- Schindler, D.W., 2012. The dilemma of controlling cultural eutrophication of lakes. *Proc. R. Soc. B Biol. Sci.* 279, 4322–4333.
- Silbs, G.M., Kromkamp, J.C., 2012. Modeling the irradiance dependency of the quantum efficiency of photosynthesis. *Limnol. Oceanogr. Methods* 10, 645–652.
- Silbs, G.M., Hecky, R.E., Smith, R.E.H., 2012. Improved estimation of carbon fixation rates from active fluorometry using spectral fluorescence in light-limited environments. *Limnol. Oceanogr. Methods* 10, 736–751.
- Silbs, G.M., Oxborough, K., Suggett, D.J., Forster, R.M., Ihnken, S., Komarek, O., Lawrenz, E., Prasil, O., Rottgers, R., Sicner, M., Simis, S.G.H., Van Dijk, M., Kromkamp, J.C., 2015. Towards autonomous measures of photosynthetic electron transport: Evaluating fluorescence-based measures of photosystem II absorption. *Limnol. Oceanogr. Methods* 13, 138–155. <http://dx.doi.org/10.1002/lom3.10014>.
- Smeltzer, E., Shambaugh, A.D., Stangel, P., 2012. Environmental change in Lake Champlain revealed by long-term monitoring. *J. Great Lakes Res.* 38, 6–18.
- Sommer, U., Adrian, R., Domis, L.D., Elser, J.J., Gaedke, U., Ibelings, B., Jeppesen, E., Lurling, M., Molinero, J.C., Mooij, W.M., van Donk, E., Winder, M., 2012. Beyond the Plankton Ecology Group (PEG) model: Mechanisms driving plankton succession. *Annu. Rev. Ecol. Syst.* 43, 429–448.
- Stern, R.W., Elser, J.J., Fee, E.J., Guildford, S.J., Chrzanowski, T.H., 1997. The light:nutrient ratio in lakes: The balance of energy and materials affects ecosystem structure and process. *Am. Nat.* 150 (6), 663–684.
- Suggett, D.J., Moore, C.M., Hickman, A.E., Geider, R.J., 2009. Interpretation of fast repetition rate (FRR) fluorescence: Signatures of phytoplankton community structure versus physiological state. *Mar. Ecol. Prog. Ser.* 376, 1–19.
- Tanzeba, S., Gan, T.Y., 2012. Potential impact of climate change on the water availability of South Saskatchewan River Basin. *Clim. Chang.* 112, 355–386.
- Tassan, S., Ferrari, G.M., 1995. An alternative approach to absorption measurements of aquatic particles retained on filters. *Limnol. Oceanogr.* 40 (8), 1358–1368.
- Taylor, B.W., Keep, C.F., Hall, R.O., Koch, B.J., Tronstad, L.M., Flecker, A.S., Ulseth, A.J., 2007. Improving the fluorometric ammonium method: matrix effects, background fluorescence, and standard additions. *J. N. Am. Benthol. Soc.* 26 (2), 167–177.
- Thrane, J.-E., Hessen, D.O., Andersen, T., 2014. The absorption of light in lakes: Negative impact of dissolved organic carbon on primary productivity. *Ecosystems* 17, 1040–1052.
- Tilman, D., 1976. Ecological competition between algae: Experimental confirmation of resource-based competition theory. *Science* 192, 463–465.
- Utermöhl, H., 1958. Zur Vervollkommen der quantitativen Phytoplankton-Methodik. *Mitt. Int. Ver. Theor. Angew. Limnol.* 9, 1–38.
- Vandergucht, D.M., Sereda, J.M., Davies, J.-M., Hudson, J.J., 2013. A comparison of phosphorus deficiency indicators with steady state phosphate in lakes. *Water Res.* 47, 1816–1826.
- Venables, H., Moore, C.M., 2010. Phytoplankton and light limitation in the Southern Ocean: Learning from high-nutrient, high-chlorophyll areas. *J. Geophys. Res. Oceans* 115, 12.
- Vogt, R.J., Sharma, S., Leavitt, P.R., 2015. Multi-decadal regulation of algal abundance and water clarity in a large continental reservoir by climatic, hydrologic and trophic processes. *J. Great Lakes Res.* <http://dx.doi.org/10.1016/j.jglr.2014.11.007> (in this issue).
- Webb, W.L., Newton, M., Starr, D., 1974. Carbon dioxide exchange of *Alnus rubra*: A mathematical model. *Oecologia* 17, 281–291.
- Webb, D.J., Burnison, B.K., Trimbee, A.M., Prepas, E.E., 1992. Comparison of chlorophyll a extractions with ethanol and dimethyl sulfoxide/acetone, and a concern about spectrophotometric phaeopigment correction. *Can. J. Fish. Aquat. Sci.* 49, 2331–2336.
- Wehr, J.D., Sheath, R.G., 2003. *Freshwater Algae Of North America: Ecology And Classification*. Academic Press, Boston, MA.
- Wetzel, R., 2001. *Limnology: Lake and River Ecosystems*. Academic Press, San Diego, CA.
- Yip, H., Johansson, J., Hudson, J., 2015. A 29-year assessment of the water clarity and chlorophyll-a concentration of a large reservoir: Investigating spatial and temporal changes using Landsat Imagery. *J. Great Lakes Res.* <http://dx.doi.org/10.1016/j.jglr.2014.11.022> (in this issue).
- Zarfi, C., Lumsdon, A.E., Berlekamp, J., Tydecks, L., Tockner, K., 2015. A global boom in hydropower dam construction. *Aquat. Sci.* 77 (1), 161–170.